UNIVERSIDAD DE CONCEPCIÓN

Centro de Investigación en Ingeniería Matemática (CI^{2}MA)

A posteriori error analysis of an augmented mixed-primal formulation for the stationary Boussinesq model

Eligio Colmenares, Gabriel N. Gatica,
Ricardo Oyarzúa

PREPRINT 2016-37

SERIE DE PRE-PUBLICACIONES

A posteriori error analysis of an augmented mixed–primal formulation for the stationary Boussinesq model*

Eligio Colmenares[†] Gabriel N. Gatica[‡] Ricardo Oyarzúa[§]

Abstract

In an earlier work of us, a new mixed finite element scheme was developed for the Boussinesq model describing natural convection. Our methodology consisted of a fixed-point strategy for the variational problem that resulted after introducing a modified pseudostress tensor and the normal component of the temperature gradient as auxiliary unknowns in the corresponding Navier–Stokes and advection–diffusion equations defining the model, respectively, along with the incorporation of parameterized redundant Galerkin terms. The well–posedness of both the continuous and discrete settings, the convergence of the associated Galerkin scheme, as well as a priori error estimates of optimal order were stated there. In this work we complement the numerical analysis of our aforementioned augmented mixed–primal method by carrying out a corresponding a posteriori error estimation in two and three dimensions. Standard arguments relying on duality techniques, and suitable Helmholtz decompositions are used to derive a global error indicator and to show its reliability. A globally efficiency property with respect to the natural norm is further proved via usual localization techniques of bubble functions. Finally, an adaptive algorithm based on a reliable, fully local and computable a posteriori error estimator induced by the aforementioned one is proposed, and its performance and effectiveness are illustrated through a few numerical examples in two dimensions.

Key words: Boussinesq model, augmented mixed–primal formulation, a posteriori error analysis, reliability, efficiency, adaptive algorithm.

Mathematics subject classifications (2000): 65N30, 65N12, 65N15, 35Q79, 80A20, 76R05, 76D07

1 Introduction

Numerical simulation of free convection processes allows to predict and analyze a large variety of situations in non–isothermal flows, mathematically described by the Boussinesq model. In a region Ω, steady state and without internal heat generation, the governing equations are given by the system

$$\begin{aligned} -\mu\,\Delta\boldsymbol{u} + (\nabla\boldsymbol{u})\,\boldsymbol{u} + \nabla p - \varphi\,\boldsymbol{g} = 0\,, \qquad \mathrm{div}(\boldsymbol{u}) = 0 \quad \text{in} \quad \Omega\,, \\ -\,\mathrm{div}(\mathbb{K}\,\nabla\varphi) + \boldsymbol{u}\cdot\nabla\varphi = 0 \quad \text{in} \quad \Omega\,, \end{aligned} \tag{1.1}$$

*This work was partially supported by CONICYT-Chile through BASAL project CMM, Universidad de Chile, project Fondecyt 11121347, and the Becas–Chile programme for foreign students; by Centro de Investigación en Ingeniería Matemática (CI^{2}MA), Universidad de Concepción; and by Universidad del Bío-Bío through DIUBB project 120808 GI/EF.

[†]Present address: CI^{2}MA and Departamento de Ingeniería Matemática, Universidad de Concepción, Casilla 160-C, Concepción, Chile, email: eligio@ci2ma.udec.cl.

[‡]CI^{2}MA and Departamento de Ingeniería Matemática, Universidad de Concepción, Casilla 160-C, Concepción, Chile, email: ggatica@ci2ma.udec.cl.

[§]GIMNAP-Departamento de Matemática, Universidad del Bío-Bío, Casilla 5-C, Concepción, Chile, and CI^{2}MA, Universidad de Concepción, Casilla 160-C, Concepción, Chile, email: royarzua@ubiobio.cl.

which describes the velocity field $\boldsymbol{u} = (u_i)_{1\le i\le n}$, the pressure p, and the temperature profile φ of a thermally driven flow with associate kinematic viscosity μ and thermal conductivity $\mathbb{K} = (k_{ij})_{1\le i,j\le n}$. Here, $\boldsymbol{g}$ is the gravitational force per unit mass and, as usual, ∇ stands for the gradient operator of scalar fields whereas the gradient, the Laplacian, and the divergence operator of the velocity $\boldsymbol{u}$ are set, respectively, as

$$\nabla \boldsymbol{u} := \left(\frac{\partial u_i}{\partial x_j}\right)_{1\le i,j\le n}, \quad \Delta \boldsymbol{u} := \mathbf{div}\,(\nabla \boldsymbol{u}) = \left(\sum_{j=1}^{n} \frac{\partial^2 u_i}{\partial x_j^2}\right)_{1\le i\le n}, \quad \text{and} \quad \operatorname{div}(\boldsymbol{u}) := \sum_{j=1}^{n} \frac{\partial u_j}{\partial x_j}.$$

In the underlying fluid flow phenomena, the velocity distribution depends on the temperature through the buoyancy term $\varphi\,\boldsymbol{g}$, and vice versa due to the convective heat transfer in the fluid velocity direction. We refer to [32, Chapters 13 and 14] for a more physical discussion of this model, its variants, as well as specific applications including geophysical contexts, and to [24, 26, 25, 29, 30] for some theoretical findings on existence of strong and/or weak solutions, considering diverse types of boundary conditions or generalized versions, such as temperature–dependent parameters.

The complexity of this coupled nonlinear problem, in addition to its applicability, has motivated the devising of numerical methods based on finite elements to approximate the corresponding solutions [3, 6, 7, 8, 9, 10, 11, 27, 28]. In this same direction, adaptive finite element algorithms have been also developed for this problem (see [1, 12, 35] and the references therein), which are particularly advantageous for situations where the convective effects become more important or the solution has a singular behaviour, for instance. On the one hand, [1] deals with the problem (1.1) in two and three dimensions with homogeneous Dirichlet conditions for both the velocity and the temperature while in [35] the problem is set in the plane but a non–homogeneous Dirichlet condition is further considered for the temperature. Both works propose a convergent, well–posed, primal finite element method, and extend the general framework of Verfürth in [33, 34] for nonlinear problems to carry out the corresponding a posteriori error analyses. The effectiveness of the adaptive method proposed by [35] is demonstrated through numerical examples. On the other hand, the authors propose in [11] a mixed finite element method in two dimensions for approximating the solution to (1.1) in polygonal domains with non-slip boundary condition for the velocity and homogeneous mixed boundary condition for the temperature. Their results show that uniform meshes lead to a slow convergence rate due to the singular behaviour of the solution near the corner points, but this is circumvented next in a subsequent work [12] where the same authors derive appropriate refinement rules to restore the quasi–optimality.

The numerical technique that will be considered in this paper is a high–order quasi-optimally convergent augmented mixed-primal finite element method proposed in an earlier work of us [8] to solve (1.1) with non–homogeneous Dirichlet boundary conditions for both the velocity and the temperature. The main features of our approach include:

1. A modified pseudostress tensor, which depends nonlinearly on the velocity, its gradient and the pressure, is introduced in the fluid equations as a new unknown. The pressure is then eliminated by its own definition from the system, and can be approximated by a simple post-process.

2. A mixed–primal formulation is considered for the heat equation, and the normal component of the temperature gradient is additionally introduced as a new unknown on the boundary. This leads us to weakly impose the corresponding Dirichlet condition for the temperature.

3. In order to place the problem in a suitable mathematical framework so that standard Hilbert spaces and (finite element) subspaces can be used in our formulations, a set of parameterized redundant Galerkin terms are included.

4. The resulting continuous variational problem and the associated discrete scheme are both well–posed, the latter is convergent, allows high–order approximation, and optimal order error estimates are derived for a suitable family of finite element subspaces.

5. Numerical experiments illustrate the good performance of the scheme and confirm the expected rate of convergence. In particular, for small values of the viscosity, our results suggested to increase the approximation order and use smaller mehsizes combined with a continuation technique in order to preserve the stability of our primal–mixed technique in an relatively affordable number of iterations (see Tables II and III in [8, Section VI]). However this certainly involves a very high computational cost, and hence the necessity of deriving suitable adaptive algorithms becomes fully justified.

According to the foregoing remarks, the aim of the present work is precisely to develop an a posteriori error analysis and propose the corresponding adaptive algorithm, which is usually of low computational cost, for improving the accuracy, the stability and the robustness of our augmented mixed–primal method when being applied to problems in which the overall approximation quality can be deteriorated by the presence of boundary layers, singularities, or complex geometries. Proceeding similarly to a previous work for a viscous flow–transport problem [2], we then begin exploiting the fixed–point strategy in which our scheme is based [9] to obtain preliminary upper bounds for the approximation error associated to the fluid and heat variables, separately, and show that deriving an a posteriori error indicator is reduced then to estimating dual–norms of residual–type expressions relative to the numerical approximation driven by our mixed–primal method. Some ideas from previous a posteriori analyses of mixed formulations for Stokes, Brinkman, and Navier–Stokes equations [21, 16, 19, 20], relying on Helmholtz decompositions and classical approximation properties of the usual Raviart–Thomas and Clement interpolant, are then extended to our setting to derive, define and state a reliable, residual–based a posteriori error estimator. The corresponding efficiency property is also shown at global level with respect to the natural norm and it essentially follows from previous results, and via usual localization techniques of bubble functions. In this latter, the nonlinear convective terms are controlled by Sobolev embeddings. Although all the analysis is carried out in two dimensions, we further point out how to extend it to the spatial case. Finally, we propose an adaptive algorithm based on a reliable, fully–local and fully–computable a posteriori error estimator induced by the aforementioned one and illustrate its performance and effectiveness through a few examples.

1.1 Outline

This paper is organized as follows. At the end of this section we set some standard notations, definitions and general assumptions. In Section 2, the mixed strong form of the Boussinesq problem considered here is recalled, and the continuous and discrete schemes are briefly described. The a posteriori error analysis of our method, which constitutes the main contribution of this work, is presented in details in Section 3. Finally, we propose an adaptive algorithm and test its effectiveness with some numerical examples in Section 4.

1.2 Preliminaries

From now on Ω is assumed to be a bounded domain in R^n ($n \in \{2,3\}$), with a polyhedral boundary Γ with outward unit normal vector $\boldsymbol{\nu}$. For a nonnegative integer m we recall the classical Sobolev space $\mathrm{W}^{m,p}(\Omega)$, equipped with its norm $\|\cdot\|_{m,p,\Omega}$, as the set of all the scalar–valued functions such that the p-th power of them and their derivatives (in the weak sense) up to order m are Lebesgue integrable in Ω. We recall that when $p = 2$, $\mathrm{W}^{m,2}(\Omega) =: \mathrm{H}^m(\Omega)$ becomes a Hilbert space with norm $\|\cdot\|_{m,\Omega}$ and seminorm $|\cdot|_{m,\Omega}$ induced by the natural definition of the corresponding inner product in $\mathrm{L}^2(\Omega)$. Obvious notations and definitions are adopted in any subdomain of Ω. In turn, with γ_0 being the usual trace operator, we let $\mathrm{H}^{1/2}(\Gamma) := \gamma_0(\mathrm{H}^1(\Omega))$ be the space of traces of functions in $\mathrm{H}^1(\Omega)$, $\mathrm{H}^{-1/2}(\Gamma)$ its dual, and denote by $\langle \cdot, \cdot \rangle_\Gamma$ the associated dual parity.

In general, given a space of scalar–valued functions M, its corresponding vectorial and tensorial extensions will be denoted by $\mathbf{M}$ and $\mathbb{M}$, respectively. Under this convention, we then denote by $\mathbb{H}(\mathbf{div};\Omega)$ the space of square integrable tensor–valued functions with divergence $\mathbf{div}$ (acting on each row) in $\mathbf{L}^2(\Omega)$, and norm $\|\cdot\|_{\mathbf{div},\Omega} = \|\cdot\|_{0,\Omega} + \|\mathbf{div}(\cdot)\|_{\mathbf{div},\Omega}$. In addition, the trace and the deviatoric part of any tensor field $\boldsymbol{\zeta} = (\zeta_{ij})_{1\le i,j\le n}$ are defined, respectively, as

$$\mathrm{tr}(\boldsymbol{\zeta}) := \sum_{i=1}^{n} \zeta_{ii}, \quad \text{and} \quad \boldsymbol{\zeta}^{\mathrm{d}} := \boldsymbol{\zeta} - \frac{1}{n}\,\mathrm{tr}(\boldsymbol{\zeta})\,\mathbb{I}\,. \tag{1.2}$$

where $\mathbb{I}$ stabds for the identity matrix. Additionally we recall the decomposition

$$\mathbb{H}(\mathbf{div};\Omega) = \mathbb{H}_0(\mathbf{div};\Omega) \oplus c\mathbb{I}\,, \tag{1.3}$$

where

$$\mathbb{H}_0(\mathbf{div};\Omega) := \left\{ \boldsymbol{\zeta} \in \mathbb{H}(\mathbf{div};\Omega) : \quad \int_\Omega \mathrm{tr}(\boldsymbol{\zeta}) = 0 \right\}. \tag{1.4}$$

To simplify, we will denote by $\|\cdot\|$, with no subscripts, the natural norm of either an element or an operator in any product functional space, and by C any positive constant independent of the mesh parameters, but that might depend on data and/or stabilization parameters, and take different values in each occurrence. As for the data, we consider that the viscosity μ is a positive constant, $\mathbb{K}$ is a uniformly positive definite tensor in $\mathbb{L}^\infty(\Omega)$, and $\boldsymbol{g} \in \mathbf{L}^\infty(\Omega)$. Finally, we complete the system (1.1) with non–homogeneous boundary conditions for the velocity and the temperature, which are denoted by $\boldsymbol{u}_D \in \mathbf{H}^{1/2}(\Gamma)$ and $\varphi_D \in \mathrm{H}^{1/2}(\Gamma)$, respectively. In particular, we suppose that $\boldsymbol{u}_D$ satisfies the usual compatibility condition

$$\int_\Gamma \boldsymbol{u}_D \cdot \boldsymbol{\nu} = 0\,. \tag{1.5}$$

2 The stationary Boussinesq model: Our approach

This section briefly describes the augmented mixed formulation considered in this work for the Boussinesq model. Firstly, in Section 2.1 we recall the strong form of the problem, and then the corresponding continuous and discrete variational formulations are discussed in Sections 2.2 and 2.3.

2.1 The equivalent strong problem

We consider from [8, Section II] the strong form of the Boussinesq problem: Find $(\boldsymbol{\sigma}, \boldsymbol{u}, \varphi)$ such that

$$\begin{gathered} \mu\,\nabla\boldsymbol{u} - (\boldsymbol{u}\otimes\boldsymbol{u})^{\mathrm{d}} = \boldsymbol{\sigma}^{\mathrm{d}}\,, \quad -\mathbf{div}(\boldsymbol{\sigma}) - \varphi\,\boldsymbol{g} = 0 \quad \text{and} \quad -\mathrm{div}(\mathbb{K}\,\nabla\varphi) + \boldsymbol{u}\cdot\nabla\varphi = 0 \quad \text{in} \quad \Omega\,, \\ \boldsymbol{u} = \boldsymbol{u}_D \quad \text{and} \quad \varphi = \varphi_D \quad \text{on} \quad \Gamma\,, \quad \text{and} \quad \int_\Omega \mathrm{tr}(\boldsymbol{\sigma} + \boldsymbol{u}\otimes\boldsymbol{u}) = 0\,, \end{gathered} \tag{2.1}$$

where $\boldsymbol{\sigma}$ is the modified pseudostress tensor defined as

$$\boldsymbol{\sigma} := \mu\,\nabla\boldsymbol{u} - (\boldsymbol{u}\otimes\boldsymbol{u}) - p\,\mathbb{I} \quad \text{in} \quad \Omega\,. \tag{2.2}$$

Note that the original system (1.1) is recovered by eliminating $\boldsymbol{\sigma}$ from the system (2.1), using that $\mathbf{div}(\boldsymbol{u}\otimes\boldsymbol{u}) = (\nabla\boldsymbol{u})\boldsymbol{u}$ when $\boldsymbol{u}$ is divergence–free in Ω, and employing the definition of the deviatoric operator (see (1.2)), and the fact that the pressure is given in terms of $\boldsymbol{u}$ and $\boldsymbol{\sigma}$ in accordance to (2.2) by

$$p \,=\, -\frac{1}{n}\,\mathrm{tr}(\,\boldsymbol{\sigma} + \boldsymbol{u}\otimes\boldsymbol{u}\,) \quad \text{in} \quad \Omega\,, \tag{2.3}$$

which along with the last statement in (2.1) imply that p has zero mean–value in Ω.

2.2 The augmented mixed-primal formulation

The weak form considered here for problem (2.1) essentially relies on three main aspects; details on its derivation are found in [8, Section III–A]:

1. From (1.3)–(1.4), problem (2.1) is firstly rewritten in a equivalent setting for approximating the $\mathbb{H}_0(\mathbf{div};\Omega)$–component, still denoted by $\boldsymbol{\sigma}$, of the pseudostress tensor, and for which the respective constant c in (1.3) is explicitly defined by
$$c \,=\, -\frac{1}{n|\Omega|}\int_\Omega \mathrm{tr}(\boldsymbol{u}\otimes\boldsymbol{u})\,.$$
2. The normal derivative of the temperature is introduced as an additional unknown on the boundary through the Lagrange multiplier $\lambda := -\mathbb{K}\nabla\varphi\cdot\boldsymbol{\nu} \in \mathrm{H}^{-1/2}(\Gamma)$, yielding the weak imposition of the Dirichlet condition for the temperature.
3. Redundant Galerkin terms weighted by parameters $\kappa_i,\ i\in\{1,2,3\}$, and which are defined from the constitutive and the equilibrium relations of the fluid equations and the Dirichlet boundary condition for the velocity (see equations (3.11) in [8]), are incorporated into the resulting variational problem.

Consequently, the underlying augmented mixed-primal formulation for (2.1) then reads as: Find $(\,\boldsymbol{\sigma},\,\boldsymbol{u},\,\varphi,\,\lambda\,) \in \mathbb{H}_0(\mathbf{div};\Omega)\times\mathbf{H}^1(\Omega)\times\mathrm{H}^1(\Omega)\times\mathrm{H}^{-1/2}(\Gamma)$ such that

$$\begin{aligned}
\mathbf{A}(\,(\boldsymbol{\sigma},\boldsymbol{u})\,,\,(\boldsymbol{\tau},\boldsymbol{v})\,) + \mathbf{B}_{\boldsymbol{u}}(\,(\boldsymbol{\sigma},\boldsymbol{u})\,,\,(\boldsymbol{\tau},\boldsymbol{v})\,) \;&=\; F_\varphi(\boldsymbol{\tau},\boldsymbol{v}) + F_D(\boldsymbol{\tau},\boldsymbol{v})\,,\\
\mathbf{a}(\varphi,\,\psi) + \mathbf{b}(\psi\,,\lambda) \;&=\; F_{\boldsymbol{u},\varphi}(\,\psi\,)\,,\\
\mathbf{b}(\varphi\,,\xi) \;&=\; G(\xi)\,,
\end{aligned} \tag{2.4}$$

for all $(\,\boldsymbol{\tau},\,\boldsymbol{v},\,\psi,\,\xi\,) \in \mathbb{H}_0(\mathbf{div};\Omega)\times\mathbf{H}^1(\Omega)\times\mathrm{H}^1(\Omega)\times\mathrm{H}^{-1/2}(\Gamma)$, where $\mathbf{A}$, $\mathbf{B}_{\boldsymbol{w}}$ (with a given $\boldsymbol{w}\in\mathbf{H}^1(\Omega)$), $\mathbf{a}$, and $\mathbf{b}$ are the bilinear forms

$$\begin{aligned}
\mathbf{A}((\boldsymbol{\sigma},\boldsymbol{u}),(\boldsymbol{\tau},\boldsymbol{v})) \,:=\, &\int_\Omega \boldsymbol{\sigma}^{\mathrm{d}} : (\,\boldsymbol{\tau}^{\mathrm{d}} - \kappa_1\nabla\boldsymbol{v}\,) + \int_\Omega (\,\mu\,\boldsymbol{u} + \kappa_2\,\mathbf{div}(\boldsymbol{\sigma})\,)\cdot\mathbf{div}(\boldsymbol{\tau})\\
&- \mu\int_\Omega \boldsymbol{v}\cdot\mathbf{div}(\boldsymbol{\sigma}) + \mu\,\kappa_1\int_\Omega \nabla\boldsymbol{u} : \nabla\boldsymbol{v} + \kappa_3\int_\Gamma \boldsymbol{u}\cdot\boldsymbol{v}\,,
\end{aligned} \tag{2.5}$$

$$\mathbf{B}_{\boldsymbol{w}}(\,(\boldsymbol{\sigma},\boldsymbol{u})\,,\,(\boldsymbol{\tau},\boldsymbol{v})\,) \,:=\, -\int_\Omega (\boldsymbol{u}\otimes\boldsymbol{w})^{\mathrm{d}} : \big(\kappa_1\nabla\boldsymbol{v} - \boldsymbol{\tau}^{\mathrm{d}}\big)\,, \tag{2.6}$$

for all $(\boldsymbol{\sigma},\boldsymbol{u})$, $(\boldsymbol{\tau},\boldsymbol{v}) \in \mathbb{H}_0(\mathbf{div};\Omega)\times\mathbf{H}^1(\Omega)$, and

$$\mathbf{a}(\varphi,\psi) \,:=\, \int_\Omega \mathbb{K}\,\nabla\varphi\cdot\nabla\psi \quad \text{and} \quad \mathbf{b}(\psi,\xi) \,:=\, \langle\,\xi,\psi\,\rangle_\Gamma\,, \tag{2.7}$$

for all $\varphi, \psi \in \mathrm{H}^1(\Omega)$ and for all $(\psi, \xi) \in \mathrm{H}^1(\Omega) \times \mathrm{H}^{-1/2}(\Gamma)$. In turn, F_φ (with a given $\varphi \in \mathrm{H}^1(\Omega)$) , F_D, $F_{\boldsymbol{u},\varphi}$ (with a given $(\boldsymbol{u}, \varphi) \in \mathbf{H}^1(\Omega) \times \mathrm{H}^1(\Omega)$), and G are the bounded linear functionals

$$F_\varphi(\boldsymbol{\tau}, \boldsymbol{v}) := \int_\Omega \varphi\, \mathbf{g} \cdot \big(\mu\, \boldsymbol{v} - \kappa_2\, \mathbf{div}(\boldsymbol{\tau})\big), \quad F_D(\boldsymbol{\tau}, \boldsymbol{v})) := \kappa_3 \int_\Gamma \boldsymbol{u}_D \cdot \boldsymbol{v} + \mu\, \langle \boldsymbol{\tau\nu}, \boldsymbol{u}_D \rangle_\Gamma, \tag{2.8}$$

$$F_{\boldsymbol{u},\varphi}(\psi) := -\int_\Omega (\boldsymbol{u} \cdot \nabla \varphi)\, \psi, \quad \text{and} \quad G(\xi) := \langle \xi, \varphi_D \rangle_\Gamma. \tag{2.9}$$

for all $(\boldsymbol{\tau}, \boldsymbol{v}) \in \mathbb{H}_0(\mathbf{div}; \Omega) \times \mathbf{H}^1(\Omega)$, for all $\psi \in \mathrm{H}^1(\Omega)$, and for all $\xi \in \mathrm{H}^{-1/2}(\Gamma)$, where κ_1, κ_2 and κ_3 are positive parameters to be chosen conveniently (see (2.10) below).

The analysis of problem (2.4) is carried out in [8, Section II], and its well-posedness is developed through a fixed-point strategy based on decoupling the fluid and heat equations and then combining the classical Banach Theorem with the Lax-Milgram Theorem and the Babŭska-Brezzi Theory. Theorem 3.9 in [8] particularly states that, under small data assumptions and a suitable choice of stabilization parameters κ_i , for instance (see equations (3.37) in [8]),

$$\kappa_1 = \mu, \qquad \kappa_2 = 1, \quad \text{and} \quad \kappa_3 = \frac{\mu^2}{2}, \tag{2.10}$$

there exists an $r_0 > 0$ such that for each $r \in (0, r_0)$ there exists a unique solution $(\boldsymbol{\sigma}, \boldsymbol{u}, \varphi, \lambda)$ to (2.4) with $(\boldsymbol{u}, \varphi) \in W(r) := \Big\{(\boldsymbol{w}, \phi) \in \mathbf{H}^1(\Omega) \times \mathrm{H}^1(\Omega) : \quad \|(\boldsymbol{w}, \phi)\| \le r\Big\}$, and satisfying further the a priori estimates

$$\begin{aligned} \|(\boldsymbol{\sigma}, \boldsymbol{u})\| &\le c_{\mathbf{S}}\big\{ r\, \|\boldsymbol{g}\|_{\infty,\Omega} + \|\boldsymbol{u}_D\|_{0,\Gamma} + \|\boldsymbol{u}_D\|_{1/2,\Gamma_D} \big\} \\ \|(\varphi, \lambda)\| &\le c_{\widetilde{\mathbf{S}}} \big\{ r\, \|\boldsymbol{u}\|_{1,\Omega} + \|\varphi_D\|_{1/2,\Gamma} \big\}, \end{aligned} \tag{2.11}$$

where $c_{\mathbf{S}}$ and $c_{\widetilde{\mathbf{S}}}$ are positive constants.

2.3 The augmented mixed-primal finite element method

Given a regular family of triangularizations $\{\mathcal{T}_h\}_{h>0}$ of $\bar{\Omega}$, each one of them made of triangles/tetrahedras T of diameter h_T and meshsize $h := \max\Big\{ h_T : \quad T \in \mathcal{T}_h \Big\}$, we let

$$\mathbb{H}_h^{\boldsymbol{\sigma}} := \mathbb{RT}_k(\mathcal{T}_h) \cap \mathbb{H}_0(\mathbf{div}; \Omega), \quad \mathbf{H}_h^{\boldsymbol{u}} := [\mathcal{P}_{k+1}(\mathcal{T}_h)]^n, \quad \text{and} \quad \mathrm{H}_h^\varphi := \mathcal{P}_{k+1}(\mathcal{T}_h) \tag{2.12}$$

be the tensorial Raviart–Thomas space of order k for approximating $\boldsymbol{\sigma}$, and the usual Lagrange finite element spaces of order $k+1$ for the velocity components and the temperature, respectively. More precisely, denoting from now on by $\mathrm{P}_k(S)$ the space of polynomials of degree $\le k$ on any subset S of R^n, we set $\mathcal{P}_{k+1}(\mathcal{T}_h) := \Big\{v \in C(\bar{\Omega}) : \quad v|_T \in \mathrm{P}_{k+1}(T) \quad \forall\, T \in \mathcal{T}_h\Big\}$. In turn, as for the unknown on the boundary, an independent triangulation $\big\{\widetilde{\Gamma}_1, \widetilde{\Gamma}_2, \ldots, \widetilde{\Gamma}_m\big\}$ of Γ (made of triangles in R^3 or straight segments in R^2) is also considered. Thus, with $\widetilde{h} := \max\limits_{j \in \{1,\ldots,m\}} |\widetilde{\Gamma}_j|$, the space approximating the Lagrange multiplier is defined as

$$\mathrm{H}_{\widetilde{h}}^\lambda := \Big\{ \xi_{\widetilde{h}} \in \mathrm{L}^2(\Gamma) : \quad \xi_{\widetilde{h}}\Big|_{\widetilde{\Gamma}_j} \in \mathrm{P}_k(\widetilde{\Gamma}_j) \quad \forall\, j \in \{1, 2, \cdots, m\} \Big\}. \tag{2.13}$$

The discrete problem based on (2.4) then reads: Find $(\boldsymbol{\sigma}_h, \boldsymbol{u}_h, \varphi_h, \lambda_{\widetilde{h}})$ satisfying

$$\begin{aligned} \mathbf{A}((\boldsymbol{\sigma}_h, \boldsymbol{u}_h), (\boldsymbol{\tau}_h, \boldsymbol{v}_h)) + \mathbf{B}_{\boldsymbol{u}_h}((\boldsymbol{\sigma}_h, \boldsymbol{u}_h), (\boldsymbol{\tau}_h, \boldsymbol{v}_h)) &= F_{\varphi_h}(\boldsymbol{\tau}_h, \boldsymbol{v}_h) + F_D(\boldsymbol{\tau}_h, \boldsymbol{v}_h) \\ \mathbf{a}(\varphi_h, \psi_h) + \mathbf{b}(\psi_h, \lambda_{\widetilde{h}}) &= F_{\boldsymbol{u}_h,\varphi_h}(\psi_h) \\ \mathbf{b}(\varphi_h, \xi_{\widetilde{h}}) &= G(\xi_{\widetilde{h}}), \end{aligned} \tag{2.14}$$

for all $(\boldsymbol{\tau}_h, \boldsymbol{v}_h, \psi_h, \xi_{\widetilde{h}}) \in \mathbb{H}_h^{\boldsymbol{\sigma}} \times \mathbf{H}_h^{\boldsymbol{u}} \times \mathrm{H}_h^{\varphi} \times \mathrm{H}_{\widetilde{h}}^{\lambda}$.

The solvability analysis of problem (2.14) follows by adapting the same arguments from the continuous case (see [8, Section IV], for details). In particular, it is showed there the existence of a positive constant C_0 and a unique solution $(\boldsymbol{\sigma}_h, \boldsymbol{u}_h, \varphi_h, \lambda_{\widetilde{h}})$ to (2.14) with $(\boldsymbol{u}_h, \varphi_h)$ in a discrete ball $W_h(r) \subseteq \mathbf{H}_h^{\boldsymbol{u}} \times \mathrm{H}_h^{\varphi}$, for all $r \in (0, r_0)$ and for all $h \leq C_0\,\widetilde{h}$, which satisfies

$$\begin{aligned} \|(\boldsymbol{\sigma}_h, \boldsymbol{u}_h)\| &\leq c_{\mathbf{S}} \left\{ r\,\|\boldsymbol{g}\|_{\infty,\Omega} + \|\boldsymbol{u}_D\|_{0,\Gamma} + \|\boldsymbol{u}_D\|_{1/2,\Gamma_D} \right\}, \\ \|(\varphi_h, \lambda_{\widetilde{h}})\| &\leq \widetilde{c}_{\widetilde{\mathbf{S}}} \left\{ r\,\|\boldsymbol{u}_h\|_{1,\Omega} + \|\varphi_D\|_{1/2,\Gamma} \right\}, \end{aligned} \tag{2.15}$$

where $c_{\mathbf{S}}$ is the same constant appearing in (2.11) and $\widetilde{c}_{\widetilde{\mathbf{S}}} > 0$ is independent of h and $\widetilde{h}$.

We also point out that the scheme (2.14) is convergent for any family of finite element spaces whenever the corresponding ones for approximating the temperature and the Lagrange multiplier are inf–sup compatible (cf. Theorem 5.5 and hypotheses **(H.1)**–**(H.2)** in [8]). Moreover, optimal–error a priori estimates are achieved when the specific subspaces defined through (2.12)–(2.13) are used (cf. [8, Theorem 5.6]).

3 A posteriori error estimation

This section provides the main contribution of this work, for which we first confine our analysis to the case where $\Omega \subseteq \mathrm{R}^2$. In Section 3.1 we introduce some preliminary notations and define a global a posteriori error estimator for the augmented primal–mixed scheme (2.14). Next, through Sections 3.1–3.2 we derive this estimator and prove its reliability, whereas in Section 3.3 we establish the corresponding efficiency estimate. Finally, in Section 3.4 we discuss the main aspects yielding the extension of our a posteriori analysis to the three–dimensional case.

3.1 The global a posteriori error estimator

We begin by introducing a few useful notations for describing local information on elements and edges. Let $\mathcal{E}_h$ be the set of edges e of $\mathcal{T}_h$, whose corresponding diameters are denoted h_e, and define

$$\mathcal{E}_h(\Omega) := \{ e \in \mathcal{E}_h : \quad e \subseteq \Omega \}, \quad \text{and} \quad \mathcal{E}_h(\Gamma) := \{ e \in \mathcal{E}_h : \quad e \subseteq \Gamma \}.$$

For each $T \in \mathcal{T}_h$, we similarly denote

$$\mathcal{E}_{h,T}(\Omega) = \{ e \subseteq \partial T : \quad e \in \mathcal{E}_h(\Omega) \} \quad \text{and} \quad \mathcal{E}_{h,T}(\Gamma) = \{ e \subseteq \partial T : \quad e \in \mathcal{E}_h(\Gamma) \}.$$

We also define unit normal and tangential vectors $\boldsymbol{\nu}$ and $\boldsymbol{s}$, respectively, on each edge $e \in \mathcal{E}_h$ by

$$\boldsymbol{\nu} := (\nu_1, \nu_2)^{\mathbf{t}} \quad \text{and} \quad \boldsymbol{s} := (-\nu_2, \nu_1)^{\mathbf{t}}.$$

Thus, the usual jump operator $[\![\,\cdot\,]\!]$ across an internal edge $e \in \mathcal{E}_h(\Omega)$ is defined for piecewise continuous matrix, vector, or scalar-valued functions $\boldsymbol{\zeta}$ as

$$[\![\boldsymbol{\zeta}]\!] = \boldsymbol{\zeta}\big|_{T_+} - \boldsymbol{\zeta}\big|_{T_-} \quad \text{where} \quad e = \partial T_+ \cap \partial T_-.$$

In addition, if $\boldsymbol{\psi} = (\psi_1, \psi_2)$ and $\boldsymbol{\zeta} = (\zeta_{i,j})_{1 \leq i,j \leq 2}$ are vector–valued and matrix-valued functions, respectively, we set the differential operators

$$\underline{\mathbf{curl}}(\boldsymbol{\psi}) := \begin{pmatrix} \dfrac{\partial \psi_1}{\partial x_2} & -\dfrac{\partial \psi_1}{\partial x_1} \\[2ex] \dfrac{\partial \psi_2}{\partial x_2} & -\dfrac{\partial \psi_2}{\partial x_1} \end{pmatrix} \quad \text{and} \quad \mathrm{curl}(\boldsymbol{\zeta}) := \begin{pmatrix} \dfrac{\partial \zeta_{12}}{\partial x_1} - \dfrac{\partial \zeta_{11}}{\partial x_2} \\[2ex] \dfrac{\partial \zeta_{22}}{\partial x_1} - \dfrac{\partial \zeta_{21}}{\partial x_2} \end{pmatrix}.$$

We now introduce the global a posteriori error estimator

$$\boldsymbol{\theta}^2 := \sum_{T\in\mathcal{T}_h} \boldsymbol{\theta}_T^2 + \|\varphi_D - \varphi_h\|_{1/2,\Gamma}^2 , \tag{3.1}$$

where $\boldsymbol{\theta}_T$ is the local indicator defined for each $T \in \mathcal{T}_h$ by

$$\begin{aligned}
\boldsymbol{\theta}_T^2 := & \|\mu \nabla \boldsymbol{u}_h - \boldsymbol{\sigma}_h^{\mathtt{d}} - (\boldsymbol{u}_h \otimes \boldsymbol{u}_h)^{\mathtt{d}}\|_{0,T}^2 + \|\mathbf{div}\, \boldsymbol{\sigma}_h + \varphi_h \, \boldsymbol{g}\|_{0,T}^2 \\
& + h_T^2 \|\mathrm{div}(\mathbb{K}\nabla\varphi_h) - \boldsymbol{u}_h \cdot \nabla\varphi_h\|_{0,T}^2 + h_T^2 \|\mathrm{curl}\{(\boldsymbol{\sigma}_h + \boldsymbol{u}_h \otimes \boldsymbol{u}_h)^{\mathtt{d}}\}\|_{0,T}^2 \\
& + \sum_{e\in\mathcal{E}_{h,T}(\Omega)} h_e \Big\{ \|[\![(\boldsymbol{\sigma}_h + \boldsymbol{u}_h \otimes \boldsymbol{u}_h)^{\mathtt{d}} \boldsymbol{s}]\!]\|_{0,e}^2 + \|[\![\mathbb{K}\nabla\varphi_h \cdot \boldsymbol{\nu}]\!]\|_{0,e}^2 \Big\} \\
& + \sum_{e\in\mathcal{E}_{h,T}(\Gamma)} \Big\{ \|\boldsymbol{u}_D - \boldsymbol{u}_h\|_{0,e}^2 + h_e \|\lambda_{\widetilde{h}} + \mathbb{K}\nabla\varphi_h \cdot \boldsymbol{\nu}\|_{0,e}^2 \Big\} \\
& + \sum_{e\in\mathcal{E}_{h,T}(\Gamma)} h_e \Big\| (\boldsymbol{\sigma}_h + \boldsymbol{u}_h \otimes \boldsymbol{u}_h)^{\mathtt{d}} \boldsymbol{s} - \mu \frac{d\boldsymbol{u}_D}{d\boldsymbol{s}} \Big\|_{0,e}^2 .
\end{aligned} \tag{3.2}$$

From the strong form of the model (cf. (2.1)) and the regularity of the continuous weak solution, the residual character of each term defining $\boldsymbol{\theta}_T$ becomes clear. In particular, observe in advance that the last term in the expression (3.2) requires the trace $\boldsymbol{u}_D$ to be more regular. This assumption will be stated and clarified below in Lemmas 3.1 and 3.10. Note further that $\boldsymbol{\theta}$ is not fully local due to the last term in (3.1). However, we show in Section 4 that $\boldsymbol{\theta}$ induces another fully computable estimator more useful for practical purposes since it particularly enables us to define an associate adaptive algorithm.

3.2 Reliability

We aim in this Section to show that $\boldsymbol{\theta}$ is a reliable a posteriori error estimator (cf. Theorem 3.1 below), for which we follow a similar procedure to the one employed in [2, Section 3.2]. More precisely, in Section 3.2.1 below we derive preliminary estimates for the approximation errors $\|(\boldsymbol{\sigma}, \boldsymbol{u}) - (\boldsymbol{\sigma}_h, \boldsymbol{u}_h)\|$ and $\|(\varphi, \lambda) - (\varphi_h, \lambda_{\widetilde{h}})\|$, separately, and combine them with a small data assumption to provide a first upper bound for the total error in terms of the dual norms of residual–type expressions that arise in our analysis. These latter will be subsequently estimated in Section 3.2.2, and we will have shown then the following result (see the end of this section).

Theorem 3.1 *Let $(\boldsymbol{\sigma}, \boldsymbol{u}, \varphi, \lambda)$ and $(\boldsymbol{\sigma}_h, \boldsymbol{u}_h, \varphi_h, \lambda_{\widetilde{h}})$ be the unique solutions to (2.4) and (2.14), respectively. Then, there exists a positive constant C_{rel}, depending on physical and stabilization parameters, but independent of h and $\widetilde{h}$, such that*

$$\|(\boldsymbol{\sigma}, \boldsymbol{u}, \varphi, \lambda) - (\boldsymbol{\sigma}_h, \boldsymbol{u}_h, \varphi_h, \lambda_{\widetilde{h}})\| \le C_{\mathrm{rel}}\, \boldsymbol{\theta} , \tag{3.3}$$

provided $\boldsymbol{u}_D \in \mathbf{H}^1(\Gamma)$ and the data are small enough (cf. Lemma 3.4).

3.2.1 Preliminary error estimates

Lemma 3.2 *There exists a positive constant $C > 0$, independent of h, such that*

$$\begin{aligned}
\|(\boldsymbol{\sigma}, \boldsymbol{u}) - (\boldsymbol{\sigma}_h, \boldsymbol{u}_h)\| \le C \Big\{ & \|\mu\nabla\boldsymbol{u}_h - (\boldsymbol{u}_h \otimes \boldsymbol{u}_h)^{\mathtt{d}} - \boldsymbol{\sigma}_h^{\mathtt{d}}\|_{0,\Omega} + \|\mathbf{div}(\boldsymbol{\sigma}_h) + \varphi_h \, \boldsymbol{g}\|_{0,\Omega} \\
& + \|\boldsymbol{u}_D - \boldsymbol{u}_h\|_{0,\Gamma} + \|\boldsymbol{g}\|_{\infty,\Omega} \|\varphi - \varphi_h\|_{1,\Omega} + \|\boldsymbol{u}_h\|_{1,\Omega} \|\boldsymbol{u} - \boldsymbol{u}_h\|_{1,\Omega} + \big\|\mathcal{R}^{\mathtt{f}}\big\| \Big\} ,
\end{aligned} \tag{3.4}$$

where $\mathcal{R}^{\mathtt{f}} : \mathbb{H}_0(\mathbf{div};\Omega) \longrightarrow \mathrm{R}$ *is the linear and bounded functional defined for each* $\boldsymbol{\tau} \in \mathbb{H}_0(\mathbf{div};\Omega)$ *by*

$$\mathcal{R}^{\mathtt{f}}(\boldsymbol{\tau}) := F_{\varphi_h}(\boldsymbol{\tau},\mathbf{0}) + F_D(\boldsymbol{\tau},\mathbf{0}) - \mathbf{A}((\boldsymbol{\sigma}_h,\boldsymbol{u}_h),(\boldsymbol{\tau},\mathbf{0})) - \mathbf{B}_{\boldsymbol{u}_h}((\boldsymbol{\sigma}_h,\boldsymbol{u}_h),(\boldsymbol{\tau},\mathbf{0}))\,, \tag{3.5}$$

and $\mathbf{A}$, $\mathbf{B}_{\boldsymbol{u}_h}$, F_{φ_h} *and* F_D *are the forms defined according to* (2.5)-(2.6) *and* (2.8).

Proof. Since $(\boldsymbol{u},0) \in W(r)$, it follows from [8, Lemma 3.3] that the bilinear form $\big(\mathbf{A} + \mathbf{B}_{\boldsymbol{u}}\big)$ is uniformly coercive on $\mathbb{H}_0(\mathbf{div};\Omega) \times \mathbf{H}^1(\Omega)$ with a positive constant $\alpha(\Omega)/2$ that depends on physical and stabilization parameters but is independent of $\boldsymbol{u}$. As a consequence of it, the following global inf–sup condition holds

$$\sup_{\substack{(\boldsymbol{\tau},\boldsymbol{v})\in\mathbb{H}_0(\mathbf{div};\Omega)\times\mathbf{H}^1(\Omega)\\(\boldsymbol{\tau},\boldsymbol{v})\neq\mathbf{0}}} \frac{\big(\mathbf{A}+\mathbf{B}_{\boldsymbol{u}}\big)(\,(\boldsymbol{\zeta},\boldsymbol{w})\,,\,(\boldsymbol{\tau},\boldsymbol{v})\,)}{\|(\boldsymbol{\tau},\boldsymbol{v})\|} \geq \frac{\alpha(\Omega)}{2}\|(\boldsymbol{\zeta},\boldsymbol{w})\|$$

for all $(\boldsymbol{\zeta},\boldsymbol{w}) \in \mathbb{H}_0(\mathbf{div};\Omega)\times\mathbf{H}^1(\Omega)$. In particular, taking $(\zeta,\boldsymbol{w}) = (\boldsymbol{\sigma},\boldsymbol{u}) - (\boldsymbol{\sigma}_h,\boldsymbol{u}_h)$ in the foregoing inequality, using the first equation of (2.4), and adding and subtracting φ_h and $\boldsymbol{u}_h$ in the forms F_φ and $\mathbf{B}_{\boldsymbol{u}}$, respectively, we find that

$$\frac{\alpha(\Omega)}{2}\|(\boldsymbol{\sigma},\boldsymbol{u}) - (\boldsymbol{\sigma}_h,\boldsymbol{u}_h)\| \leq \sup_{\substack{(\boldsymbol{\tau},\boldsymbol{v})\in\mathbb{H}_0(\mathbf{div};\Omega)\times\mathbf{H}^1(\Omega)\\(\boldsymbol{\tau},\boldsymbol{v})\neq\mathbf{0}}} \frac{\mathcal{Q}^{\mathtt{f}}(\boldsymbol{\tau},\boldsymbol{v}) + \mathcal{R}^{\mathtt{f}}(\boldsymbol{\tau}) + \mathcal{S}^{\mathtt{f}}(\boldsymbol{v})}{\|(\boldsymbol{\tau},\boldsymbol{v})\|}\,,$$

which yields

$$\|(\boldsymbol{\sigma},\boldsymbol{u}) - (\boldsymbol{\sigma}_h,\boldsymbol{u}_h)\| \leq C\,\Big\{\|\mathcal{Q}^{\mathtt{f}}\| + \|\mathcal{R}^{\mathtt{f}}\| + \|\mathcal{S}^{\mathtt{f}}\|\Big\}\,, \tag{3.6}$$

where $\mathcal{R}^{\mathtt{f}} \in \mathbb{H}_0(\mathbf{div};\Omega)'$ is already given by (3.5), whereas $\mathcal{Q}^{\mathtt{f}} \in \big(\mathbb{H}_0(\mathbf{div};\Omega)\times\mathbf{H}^1(\Omega)\big)'$ and $\mathcal{S}^{\mathtt{f}} \in \mathbf{H}^1(\Omega)'$ are defined, respectively, as

$$\mathcal{Q}^{\mathtt{f}}(\boldsymbol{\tau},\boldsymbol{v}) := F_{\varphi-\varphi_h}(\boldsymbol{\tau},\boldsymbol{v}) - \mathbf{B}_{\boldsymbol{u}-\boldsymbol{u}_h}((\boldsymbol{\sigma}_h,\boldsymbol{u}_h),(\boldsymbol{\tau},\boldsymbol{v}))\,,$$

and

$$\mathcal{S}^{\mathtt{f}}(\boldsymbol{v}) := F_{\varphi_h}(\mathbf{0},\boldsymbol{v}) + F_D(\mathbf{0},\boldsymbol{v}) - \mathbf{A}((\boldsymbol{\sigma}_h,\boldsymbol{u}_h),(\mathbf{0},\boldsymbol{v})) - \mathbf{B}_{\boldsymbol{u}_h}((\boldsymbol{\sigma}_h,\boldsymbol{u}_h),(\mathbf{0},\boldsymbol{v}))\,.$$

Next, according to the definitions of all the forms involved, and applying Cauchy-Schwarz's inequality, we readily obtain

$$\|\mathcal{Q}^{\mathtt{f}}\| \leq (\mu+\kappa_2)\,\|\boldsymbol{g}\|_{\infty,\Omega}\,\|\varphi-\varphi_h\|_{1,\Omega} + (1+\kappa_1)\,\|\boldsymbol{u}_h\|_{1,\Omega}\,\|\boldsymbol{u}-\boldsymbol{u}_h\|_{1,\Omega} \tag{3.7}$$

and

$$\|\mathcal{S}^{\mathtt{f}}\| \leq \kappa_1\,\|\mu\,\nabla\boldsymbol{u}_h - (\boldsymbol{u}_h\otimes\boldsymbol{u}_h)^{\mathtt{d}} - \boldsymbol{\sigma}_h^{\mathtt{d}}\|_{0,\Omega} + \mu\,\|\mathbf{div}(\boldsymbol{\sigma}_h) + \varphi_h\,\boldsymbol{g}\|_{0,\Omega} + \kappa_3\,\|\boldsymbol{u}_D - \boldsymbol{u}_h\|_{0,\Gamma}\,. \tag{3.8}$$

In this way, replacing (3.7) and (3.8) back into (3.6), we arrive at the required estimate (3.4). □

We remark here that the right-hand side of (3.4) depends on the expression $\|\boldsymbol{u}-\boldsymbol{u}_h\|_{1,\Omega}$, which is part of the total error that is being estimated. This evident vicious circle will be solved later on by assuming sufficiently small data.

We now derive an analogous preliminary bound for the error associated to the heat variables.

Lemma 3.3 *There exists a positive constant $C > 0$, independent of h and $\widetilde{h}$, such that*

$$\begin{aligned} \|(\varphi,\lambda) \,-\, (\varphi_h,\lambda_{\widetilde{h}})\| \,\le\, C\Big\{ \|\varphi\|_{1,\Omega}\,\|\boldsymbol{u}-\boldsymbol{u}_h\|_{1,\Omega} \,+\, \|\boldsymbol{u}_h\|_{1,\Omega}\,\|\varphi-\varphi_h\|_{1,\Omega} \\ +\, \|\varphi_D-\varphi_h\|_{1/2,\Gamma} \,+\, \|\mathcal{R}^{\mathrm{h}}\| \Big\}. \end{aligned} \tag{3.9}$$

where $\mathcal{R}^{\mathrm{h}} : \mathrm{H}^1(\Omega) \longrightarrow \mathrm{R}$ is the linear and bounded functional defined as

$$\mathcal{R}^{\mathrm{h}}(\psi) \,=\, F_{\boldsymbol{u}_h,\varphi_h}(\psi) \,-\, \mathbf{a}(\varphi_h,\psi) \,-\, \mathbf{b}(\psi,\lambda_{\widetilde{h}}) \tag{3.10}$$

with $\mathbf{a}$, $\mathbf{b}$ and $F_{\boldsymbol{u}_h,\varphi_h}$ given by (2.7) and (2.9).

Proof. We proceed similarly to the proof of Lemma 3.2. Indeed, we first observe that the well–posedness of the heat uncoupled problem (second and third equations in (2.4)) and the corresponding continuous dependence result (cf. [8, Lemma 3.4]) imply the existence of a positive constant C such that the following global inf-sup condition holds

$$\sup_{\substack{(\psi,\xi)\in \mathrm{H}^1(\Omega)\times \mathrm{H}^{-1/2}(\Gamma)\\ (\psi,\xi)\neq \mathbf{0}}} \frac{\mathbf{a}(\phi,\psi) \,+\, \mathbf{b}(\psi,\eta) \,+\, \mathbf{b}(\phi,\xi)}{\|(\psi,\xi)\|} \ge C\,\|(\phi,\eta)\| \quad \forall\,(\psi,\eta)\in \mathrm{H}^1(\Omega)\times \mathrm{H}^{-1/2}(\Gamma)\,.$$

Then, applying the foregoing inequality to the error $(\phi,\eta) \,=\, (\varphi,\lambda) \,-\, (\varphi_h,\lambda_{\widetilde{h}})$, using the second and third equations of (2.4), and adding and subtracting $\boldsymbol{u}_h$ and φ_h within the definition of the functional $F_{\boldsymbol{u},\varphi}$, we deduce that

$$C\,\|(\varphi,\lambda) \,-\, (\varphi_h,\lambda_{\widetilde{h}})\| \,\le \sup_{\substack{(\psi,\xi)\in \mathrm{H}^1(\Omega)\times \mathrm{H}^{-1/2}(\Gamma)\\ (\psi,\xi)\neq \mathbf{0}}} \frac{\mathcal{Q}^{\mathrm{h}}(\psi) \,+\, \mathcal{R}^{\mathrm{h}}(\psi) \,+\, \mathcal{S}^{\mathrm{h}}(\xi)}{\|(\psi,\xi)\|}\,,$$

which gives

$$\|(\varphi,\lambda) \,-\, (\varphi_h,\lambda_{\widetilde{h}})\| \,\le\, C\Big\{ \|\mathcal{Q}^{\mathrm{h}}\| \,+\, \|\mathcal{R}^{\mathrm{h}}\| \,+\, \|\mathcal{S}^{\mathrm{h}}\| \Big\}, \tag{3.11}$$

where $\mathcal{R}^{\mathrm{h}} \in \mathrm{H}^1(\Omega)'$ has already been defined (cf. (3.10)), and $\mathcal{Q}^{\mathrm{h}} \in \mathrm{H}^1(\Omega)'$ and $\mathcal{S}^{\mathrm{h}} \in \mathrm{H}^{-1/2}(\Gamma)'$ are given, respectively, by

$$\mathcal{Q}^{\mathrm{h}}(\psi) \,:=\, F_{\boldsymbol{u}-\boldsymbol{u}_h,\varphi}(\psi) \,+\, F_{u_h,\varphi-\varphi_h}(\psi)\,,$$

and

$$\mathcal{S}^{\mathrm{h}}(\xi) \,:=\, G(\xi) \,-\, \mathbf{b}(\varphi_h,\xi) \,=\, \langle \xi, \varphi_D-\varphi_h\rangle_\Gamma\,.$$

Then, applying Hölder's inequality, the continuity of the injection $\mathrm{H}^1(\Omega) \hookrightarrow \mathrm{L}^4(\Omega)$ and its vector version, and the duality pairing between $\mathrm{H}^{-1/2}(\Gamma)$ and $\mathrm{H}^{1/2}(\Gamma)$, we obtain

$$\|\mathcal{Q}^{\mathrm{h}}\| \,\le\, C\Big\{ \|\varphi\|_{1,\Omega}\,\|\boldsymbol{u}-\boldsymbol{u}_h\|_{1,\Omega} \,+\, \|\boldsymbol{u}_h\|_{1,\Omega}\,\|\varphi-\varphi_h\|_{1,\Omega} \Big\} \tag{3.12}$$

and

$$\|\mathcal{S}^{\mathrm{h}}\| \,\le\, \|\varphi_D-\varphi_h\|_{1/2,\Gamma}\,. \tag{3.13}$$

Finally, replacing (3.12) and (3.13) back into (3.11), we get (3.9) and end the proof. □

With the help of the previous Lemmas we derive now a preliminary upper bound for the total error. Indeed, from (3.4) and (3.9), we easily find

$$\|(\boldsymbol{\sigma},\boldsymbol{u},\varphi,\lambda) - (\boldsymbol{\sigma}_h,\boldsymbol{u}_h,\varphi_h,\lambda_{\widetilde{h}})\| \le C\Big\{ \|\mu\nabla\boldsymbol{u}_h - (\boldsymbol{u}_h\otimes\boldsymbol{u}_h)^{\mathtt{d}} - \boldsymbol{\sigma}_h^{\mathtt{d}}\|_{0,\Omega}$$
$$+ \|\mathbf{div}\,\boldsymbol{\sigma}_h + \varphi_h\,\boldsymbol{g}\|_{0,\Omega} + \|\boldsymbol{u}_D - \boldsymbol{u}_h\|_{0,\Gamma} + \|\varphi_D - \varphi_h\|_{1/2,\Gamma} + \big\|\mathcal{R}^{\mathtt{f}}\big\| + \big\|\mathcal{R}^{\mathtt{h}}\big\|$$
$$+ \Big(\|\boldsymbol{g}\|_{\infty,\Omega} + 2\,\|\boldsymbol{u}_h\|_{1,\Omega} + \|\varphi\|_{1,\Omega}\Big)\|(\boldsymbol{\sigma},\boldsymbol{u},\varphi,\lambda) - (\boldsymbol{\sigma}_h,\boldsymbol{u}_h,\varphi_h,\lambda_{\widetilde{h}})\|\Big\}.$$

Then, using the a priori bounds for $\boldsymbol{u}_h$ and φ in accordance to (2.11) and (2.15), respectively, we deduce that the factor multiplying the total error at the right–hand side of the latter expression can be bounded by data as

$$\begin{aligned} &\|\boldsymbol{g}\|_{\infty,\Omega} + 2\,\|\boldsymbol{u}_h\|_{1,\Omega} + \|\varphi\|_{1,\Omega} \\ &\le (r+1)\,(2 + r c_{\mathbf{S}} + c_{\widetilde{\mathbf{S}}})\Big\{ \|\boldsymbol{g}\|_{\infty,\Omega} + \|\boldsymbol{u}_D\|_{0,\Gamma} + \|\boldsymbol{u}_D\|_{1/2,\Gamma} + \|\varphi_D\|\Big\} := C(\boldsymbol{g},\boldsymbol{u}_D,\varphi_D)\,. \end{aligned} \tag{3.14}$$

In light of this, we immediately state the following result.

Lemma 3.4 *Assume that the data is sufficiently small so that the constant $C(\boldsymbol{g},\boldsymbol{u}_D,\varphi_D)$ given by (3.14) is such that $C(\boldsymbol{g},\boldsymbol{u}_D,\varphi_D) \le 1/2$. Then, the total error satisfies*

$$\|(\boldsymbol{\sigma},\boldsymbol{u},\varphi,\lambda) - (\boldsymbol{\sigma}_h,\boldsymbol{u}_h,\varphi_h,\lambda_{\widetilde{h}})\| \le C\Big\{ \|\mu\nabla\boldsymbol{u}_h - (\boldsymbol{u}_h\otimes\boldsymbol{u}_h)^{\mathtt{d}} - \boldsymbol{\sigma}_h^{\mathtt{d}}\|_{0,\Omega}$$
$$+ \|\mathbf{div}\,\boldsymbol{\sigma}_h + \varphi_h\,\boldsymbol{g}\|_{0,\Omega} + \|\boldsymbol{u}_D - \boldsymbol{u}_h\|_{0,\Gamma} + \|\varphi_h - \varphi_D\|_{1/2,\Gamma} + \big\|\mathcal{R}^{\mathtt{f}}\big\| + \big\|\mathcal{R}^{\mathtt{h}}\big\|\Big\},$$

where C depends on μ and κ_i, $i\in\{1,2,3\}$, but is independent of h and $\widetilde{h}$ (cf. Lemmas 3.2 and 3.3), and $\mathcal{R}^{\mathtt{f}}$ and $\mathcal{R}^{\mathtt{h}}$ are the linear and bounded functionals defined by (3.5) and (3.10), respectively.

According to this result, and in order to complete the derivation of our a posteriori error estimator $\boldsymbol{\theta}$, we now need to obtain suitable upper bounds for the norms of the functionals $\mathcal{R}^{\mathtt{f}}$ and $\mathcal{R}^{\mathtt{h}}$ (note here that the choice of the superscripts `f` and `h` have been motivated by the words `fluid` and `heat`). Incidentally, from the discrete problem (2.14) we first observe that

$$\mathcal{R}^{\mathtt{f}}(\boldsymbol{\tau}_h) = 0 \quad \forall\,\boldsymbol{\tau}_h\in\mathbb{H}_h^{\boldsymbol{\sigma}}, \qquad \text{and} \qquad \mathcal{R}^{\mathtt{h}}(\psi_h) = 0 \quad \forall\,\psi_h\in\mathrm{H}_h^{\varphi},$$

which essentially says that these functionals are the corresponding residuals in the spaces $\mathbb{H}_0(\mathbf{div};\Omega)$ and $\mathrm{H}^1(\Omega)$, respectively, relative to the numerical approximation driven by our augmented mixed–primal scheme. As a result, we certainly can write

$$\big\|\mathcal{R}^{\mathtt{f}}\big\| := \sup_{\substack{\boldsymbol{\tau}\in\mathbb{H}_0(\mathbf{div};\Omega)\\ \boldsymbol{\tau}\neq\mathbf{0}}} \frac{\mathcal{R}^{\mathtt{f}}(\boldsymbol{\tau}-\boldsymbol{\tau}_h^{\mathcal{R}})}{\|\boldsymbol{\tau}\|_{\mathbf{div},\Omega}}\,, \quad \text{and} \quad \big\|\mathcal{R}^{\mathtt{h}}\big\| := \sup_{\substack{\psi\in\mathrm{H}^1(\Omega)\\ \psi\neq 0}} \frac{\mathcal{R}^{\mathtt{h}}(\psi-\psi_h^{\mathcal{R}})}{\|\psi\|_{1,\Omega}}\,, \tag{3.15}$$

where $\boldsymbol{\tau}_h^{\mathcal{R}}\in\mathbb{H}_h^{\boldsymbol{\sigma}}$ and $\psi_h^{\mathcal{R}}\in\mathrm{H}_h^{\varphi}$ are going to be suitably chosen later on.

3.2.2 Estimation of $\|\mathcal{R}^{\mathtt{f}}\|$ and $\|\mathcal{R}^{\mathtt{h}}\|$

This section is devoted to the estimation of $\|\mathcal{R}^{\mathtt{f}}\|$ and $\|\mathcal{R}^{\mathtt{h}}\|$ by using some techniques from previous works [2, 21, 18, 16, 19, 20]. In particular, a stable Helmholtz decomposition of the space $\mathbb{H}_0(\mathbf{div};\Omega)$, the classical properties of the usual Raviart–Thomas interpolator, and the approximation properties of the Clément interpolation operator will be employed for this purpose. We begin recalling some of the required properties.

Lemma 3.5 ([4] Section III.3.3, [14] Section 3.4.4, [31] Lemma 1.130) *Given an integer $k \geq 0$, we let $\Pi_h^k : \mathbb{H}^1(\Omega) \longrightarrow \mathbb{RT}_k(\mathcal{T}_h)$ be the usual Raviart–Thomas interpolation operator. Then,*

i) for each $\boldsymbol{\zeta} \in \mathbb{H}^m(\Omega)$, with $1 \leq m \leq k+1$, there holds

$$\|\boldsymbol{\zeta} - \Pi_h^k(\boldsymbol{\zeta})\|_{0,T} \leq C\, h_T^m\, |\boldsymbol{\zeta}|_{m,T} \quad \forall\, T \in \mathcal{T}_h\,. \tag{3.16a}$$

ii) for each $\boldsymbol{\zeta} \in \mathbb{H}^1(\Omega)$ such that $\mathbf{div}(\boldsymbol{\zeta}) \in \mathbf{H}^m(\Omega)$, with $0 \leq m \leq k+1$, there holds

$$\|\mathbf{div}(\boldsymbol{\zeta} - \Pi_h^k(\boldsymbol{\zeta}))\|_{0,T} \leq C\, h_T^m\, |\mathbf{div}\,\boldsymbol{\zeta}|_{m,T} \quad \forall\, T \in \mathcal{T}_h\,. \tag{3.16b}$$

iii) for each $\boldsymbol{\zeta} \in \mathbb{H}^1(\Omega)$ there holds

$$\|\boldsymbol{\zeta}\,\boldsymbol{\nu} - \Pi_h^k(\boldsymbol{\zeta})\,\boldsymbol{\nu}\|_{0,e} \leq C\, h_e^{1/2}\, |\boldsymbol{\zeta}|_{1,T_e}\,, \tag{3.16c}$$

where T_e is the element of $\mathcal{T}_h$ having e as an edge.

Lemma 3.6 ([5]) *Let $\mathrm{X}_h = \Big\{ v_h \in \mathrm{C}(\bar{\Omega}) :\ v_h\big|_T \in \mathrm{P}_1(T) \quad \forall\, T \in \mathcal{T}_h \Big\}$, and let $I_h : \mathrm{H}^1(\Omega) \to \mathrm{X}_h$ be the usual Clément interpolation operator. Then, there holds*

$$\|v - I_h v\|_{0,T} \leq C\, h_T\, |v|_{1,\Delta(T)} \quad \forall\, T \in \mathcal{T}_h\,, \quad \text{and} \quad \|v - I_h v\|_{0,e} \leq C\, h_e^{1/2}\, \|v\|_{1,\Delta(e)} \quad \forall\, e \in \mathcal{E}_h\,,$$

where $\Delta(T)$ and $\Delta(e)$ are the unions of all elements intersecting with T and e, respectively.

The following result provides a stable Helmholtz decomposition of the space $\mathbb{H}_0(\mathbf{div};\Omega)$. Its proof can be found in [21, Lemma 3.7].

Lemma 3.7 *For each $\boldsymbol{\tau} \in \mathbb{H}_0(\mathbf{div};\Omega)$ there exists $\boldsymbol{z} \in \mathbf{H}^2(\Omega)$ and $\boldsymbol{\phi} \in \mathbf{H}^1(\Omega)$ such that*

$$\boldsymbol{\tau} = \nabla \boldsymbol{z} + \underline{\mathbf{curl}}(\boldsymbol{\phi}) \quad \text{in} \quad \Omega\,, \quad \text{and} \quad \|\boldsymbol{z}\|_{2,\Omega} + \|\boldsymbol{\phi}\|_{1,\Omega} \leq C\, \|\boldsymbol{\tau}\|_{\mathbf{div},\Omega}\,. \tag{3.17}$$

As a consequence of Lemma 3.7, we can rewrite $\mathcal{R}^{\mathtt{f}}$ as follows.

Lemma 3.8 *Given $\boldsymbol{\tau} \in \mathbb{H}_0(\mathbf{div};\Omega)$, let $(\boldsymbol{z},\boldsymbol{\phi}) \in \mathbf{H}^2(\Omega) \times \mathbf{H}^1(\Omega)$ be the components of its associated Helmholtz decomposition (cf. Lemma 3.7). Then there holds*

$$\mathcal{R}^{\mathtt{f}}(\boldsymbol{\tau}) = \mathcal{R}_1^{\mathtt{f}}(\nabla \boldsymbol{z}) + \mathcal{R}_2^{\mathtt{f}}(\underline{\mathbf{curl}}(\boldsymbol{\phi}))\,, \tag{3.18}$$

where

$$\begin{aligned} \mathcal{R}_1^{\mathtt{f}}(\nabla \boldsymbol{z}) &= \int_\Omega \big(\mu\, \nabla \boldsymbol{u}_h - \boldsymbol{\sigma}_h^{\mathtt{d}} - (\boldsymbol{u}_h \otimes \boldsymbol{u}_h)^{\mathtt{d}} \big) : \nabla \boldsymbol{z} \\ &- \kappa_2 \int_\Omega (\mathbf{div}(\boldsymbol{\sigma}_h) + \varphi_h\, \boldsymbol{g}) \cdot \mathbf{div}(\nabla \boldsymbol{z}) + \mu \langle \nabla \boldsymbol{z}\, \boldsymbol{\nu}, \boldsymbol{u}_D - \boldsymbol{u}_h \rangle_\Gamma\,, \end{aligned} \tag{3.19}$$

and

$$\mathcal{R}_2^{\mathtt{f}}(\underline{\mathbf{curl}}(\boldsymbol{\phi})) := -\int_\Omega \big(\boldsymbol{\sigma}_h + (\boldsymbol{u}_h \otimes \boldsymbol{u}_h) \big)^{\mathtt{d}} : \underline{\mathbf{curl}}(\boldsymbol{\phi}) + \mu\, \langle \underline{\mathbf{curl}}(\boldsymbol{\phi})\, \boldsymbol{\nu}\,, \boldsymbol{u}_D \rangle_\Gamma\,. \tag{3.20}$$

Proof. Replacing $\boldsymbol{\tau} = \nabla \boldsymbol{z} + \underline{\mathbf{curl}}(\boldsymbol{\phi})$ in the definition of $\mathcal{R}^{\mathtt{f}}$ (cf. (3.5)), using there that $\mathbf{div}\,\underline{\mathbf{curl}} = \mathbf{0}$, and then integrating by parts the first two terms on the right hand side below, we get

$$\begin{aligned}
\mathcal{R}^{\mathtt{f}}(\boldsymbol{\tau}) &= \mu\,\langle (\nabla \boldsymbol{z})\,\boldsymbol{\nu}\,,\boldsymbol{u}_D\,\rangle_\Gamma - \mu \int_\Omega \boldsymbol{u}_h \cdot \mathbf{div}(\nabla \boldsymbol{z}) - \int_\Omega \big(\boldsymbol{\sigma}_h + (\boldsymbol{u}_h \otimes \boldsymbol{u}_h)\big)^{\mathtt{d}} : \nabla \boldsymbol{z} \\
&\quad - \kappa_2 \int_\Omega (\mathbf{div}(\boldsymbol{\sigma}_h) + \varphi_h\,\boldsymbol{g}) \cdot \mathbf{div}(\nabla \boldsymbol{z}\,) - \int_\Omega \big(\boldsymbol{\sigma}_h + (\boldsymbol{u}_h \otimes \boldsymbol{u}_h)\big)^{\mathtt{d}} : \underline{\mathbf{curl}}(\boldsymbol{\phi}) + \mu\,\langle\,\underline{\mathbf{curl}}(\boldsymbol{\phi})\,\boldsymbol{\nu}\,,\boldsymbol{u}_D\,\rangle_\Gamma \\
&= \int_\Omega \big(\mu\,\nabla \boldsymbol{u}_h - \boldsymbol{\sigma}_h^{\mathtt{d}} - (\boldsymbol{u}_h \otimes \boldsymbol{u}_h)^{\mathtt{d}}\big) : \nabla \boldsymbol{z} - \kappa_2 \int_\Omega (\mathbf{div}(\boldsymbol{\sigma}_h) + \varphi_h\,\boldsymbol{g}) \cdot \mathbf{div}(\nabla \boldsymbol{z}\,) \\
&\quad + \mu \langle \nabla \boldsymbol{z}\,\boldsymbol{\nu}, \boldsymbol{u}_D - \boldsymbol{u}_h \rangle_\Gamma - \int_\Omega \big(\boldsymbol{\sigma}_h + (\boldsymbol{u}_h \otimes \boldsymbol{u}_h)\big)^{\mathtt{d}} : \underline{\mathbf{curl}}(\boldsymbol{\phi}) + \mu\,\langle\,\underline{\mathbf{curl}}(\boldsymbol{\phi})\,\boldsymbol{\nu}\,,\boldsymbol{u}_D\,\rangle_\Gamma\,,
\end{aligned}$$

which gives (3.18) with $\mathcal{R}_1^{\mathtt{f}}(\nabla \boldsymbol{z})$ and $\mathcal{R}_2^{\mathtt{f}}(\underline{\mathbf{curl}}(\boldsymbol{\phi}))$ defined by (3.19) and (3.20). □

As pointed out at the end of the previous section, (3.15) suggests that estimating $\|\mathcal{R}^{\mathtt{f}}\|$ requires to use a suitable discrete element $\boldsymbol{\tau}_h^{\mathcal{R}}$. In turn, the foregoing lemma further says that this estimation can be performed by bounding the functionals $\mathcal{R}_i^{\mathtt{f}}$, $i \in \{1, 2\}$. These facts and the Helmholtz decomposition provided by Lemma 3.7 clearly induce then to define, for each $\boldsymbol{\tau} \in \mathbb{H}_0(\mathbf{div}; \Omega)$,

$$\boldsymbol{\tau}_h^{\mathcal{R}} := \Pi_h^k(\nabla \boldsymbol{z}) + \underline{\mathbf{curl}}(I_h \boldsymbol{\phi}) + c\,\mathbb{I}\,, \quad \text{where } c \in \mathrm{R} \text{ is such that } \int_\Omega \mathrm{tr}(\boldsymbol{\tau}_h) = 0\,, \tag{3.21}$$

Π_h^k is the Raviart–Thomas interpolant operator (cf. Lemma 3.5), and $I_h \boldsymbol{\phi}$ is the componentwise Clément interpolant of $\boldsymbol{\phi}$ (cf. Lemma 3.6). Observe also from the definition of $\mathcal{R}^{\mathtt{f}}$ in (3.5), and the compatibility condition (1.5) that $\mathcal{R}^{\mathtt{f}}(c\,\mathbb{I}) = 0$, so that according to the identity (3.18), it follows

$$\mathcal{R}^{\mathtt{f}}(\boldsymbol{\tau} - \boldsymbol{\tau}_h^{\mathcal{R}}) = \mathcal{R}_1^{\mathtt{f}}(\nabla \boldsymbol{z} - \Pi_h^k(\nabla \boldsymbol{z})) + \mathcal{R}_2^{\mathtt{f}}(\underline{\mathbf{curl}}(\boldsymbol{\phi} - I_h \boldsymbol{\phi}))\,, \tag{3.22}$$

which shows that the estimation of $\|\mathcal{R}^{\mathtt{f}}\|$ (cf. (3.15)) relies now on the well–known approximation properties of the Raviart-Thomas and Clément interpolants, and this in turn justifies why we propose to use the Helmholtz decomposition (3.17) and its so-called discrete version (3.21).

Thus, we focus next on estimating $\mathcal{R}_i^{\mathtt{f}}$ given by (3.19)–(3.20), separately. Regarding the expression $\mathcal{R}_1^{\mathtt{f}}$ we have the following result.

Lemma 3.9 *There exists a positive constant C, independent of h, such that*

$$\begin{aligned}
\big|\mathcal{R}_1^{\mathtt{f}}(\nabla \boldsymbol{z} - \Pi_h^k(\nabla \boldsymbol{z}))\big| &\le C \Bigg\{ \sum_{T \in \mathcal{T}_h} h_T^2\,\|\mu\,\nabla \boldsymbol{u}_h - \boldsymbol{\sigma}_h^{\mathtt{d}} - (\boldsymbol{u}_h \otimes \boldsymbol{u}_h)^{\mathtt{d}}\|_{0,T}^2 \\
&+ \sum_{T \in \mathcal{T}_h} \|\mathbf{div}\,\boldsymbol{\sigma}_h + \varphi_h\,\boldsymbol{g}\|_{0,T}^2 + \sum_{e \in \mathcal{E}_h(\Gamma)} h_e\,\|\boldsymbol{u}_D - \boldsymbol{u}_h\|_{0,e}^2 \Bigg\}^{1/2} \|\boldsymbol{\tau}\|_{\mathbf{div},\Omega}\,.
\end{aligned} \tag{3.23}$$

Proof. From the Cauchy-Schwarz inequality and the approximation property (3.16a) with $m = 1$, we have on one hand that

$$\begin{aligned}
&\left|\int_T \big(\mu\,\nabla \boldsymbol{u}_h - \boldsymbol{\sigma}_h^{\mathtt{d}} - (\boldsymbol{u}_h \otimes \boldsymbol{u}_h)^{\mathtt{d}}\big) : (\nabla \boldsymbol{z} - \Pi_h^k(\nabla \boldsymbol{z})\,)\right| \\
&\qquad \le \quad C\,h_T \left\|\mu\,\nabla \boldsymbol{u}_h - \boldsymbol{\sigma}_h^{\mathtt{d}} - (\boldsymbol{u}_h \otimes \boldsymbol{u}_h)^{\mathtt{d}}\right\|_{0,T} |\nabla \boldsymbol{z}|_{1,T}\,.
\end{aligned}$$

and from (3.16b) with $\boldsymbol{\zeta} = \nabla \boldsymbol{z}$ and $m = 0$, and recalling that $\mathbf{div}\,\nabla \boldsymbol{z} = \mathbf{div}\,\boldsymbol{\tau}$ we also find that

$$\left|\kappa_2 \int_T (\mathbf{div}\,\boldsymbol{\sigma}_h + \varphi_h\,\boldsymbol{g}) \cdot \mathbf{div}(\,\nabla \boldsymbol{z} - \Pi_h^k(\nabla \boldsymbol{z})\,)\right| \le C\,\kappa_2\,\|\mathbf{div}\,\boldsymbol{\sigma}_h + \varphi_h\,\boldsymbol{g}\|_{0,T}\,\|\mathbf{div}\,\boldsymbol{\tau}\|_{0,T}\,.$$

In turn, thanks to (3.16c) we readily obtain

$$\left| \mu\langle \nabla \boldsymbol{z}\, \boldsymbol{\nu} \,-\, \Pi_h^k(\nabla \boldsymbol{z})\, \boldsymbol{\nu}, \boldsymbol{u}_D \,-\, \boldsymbol{u}_h \rangle_\Gamma \right| \,\leq\, C \left\{ \sum_{e\in\mathcal{E}_h(\Gamma)} h_e \, \|\boldsymbol{u}_D - \boldsymbol{u}_h\|_{0,e}^2 \right\}^{1/2} |\nabla \boldsymbol{z}|_{1,\Omega} \,.$$

In this way, combining these upper bounds in the definition of $\mathcal{R}_1^{\mathbf{f}}$ along with the Cauchy-Schwarz inequality, the regularity of the mesh $\mathcal{T}_h$, and the fact that $\|\nabla \boldsymbol{z}\|_{1,\Omega} \,\leq\, \|\boldsymbol{z}\|_{2,\Omega} \,\leq\, C\,\|\boldsymbol{\tau}\|_{\mathbf{div},\Omega}$ (cf. (3.17)), yields (3.23) and finishes the proof. □

Now we use similar arguments to those in [21, Lemma 3.9], [18, Lemma 6], [19, Lemma 4.3] and [20, Lemma 4.3] for estimating $\mathcal{R}_2^{\mathbf{f}}$, which requires an additional regularity of the trace $\boldsymbol{u}_D$.

Lemma 3.10 *Assume that $\boldsymbol{u}_D \in \mathbf{H}^1(\Gamma)$. Then, there exists a positive constant $C > 0$, independent of h, such that*

$$\begin{aligned} \left|\mathcal{R}_2^{\mathbf{f}}(\underline{\mathbf{curl}}(\boldsymbol{\phi} - I_h\boldsymbol{\phi}))\right| \,\leq\, C \Bigg\{ & \sum_{T\in\mathcal{T}_h} h_T^2 \, \|\mathrm{curl}\big((\boldsymbol{\sigma}_h \,+\, \boldsymbol{u}_h\otimes\boldsymbol{u}_h)^{\mathtt{d}}\big)\|_{0,T}^2 \\ & + \sum_{e\in\mathcal{E}_h(\Omega)} h_e \, \| [\![(\boldsymbol{\sigma}_h \,+\, \boldsymbol{u}_h\otimes\boldsymbol{u}_h)^{\mathtt{d}}\, \boldsymbol{s}]\!] \|_{0,e}^2 \\ & + \sum_{e\in\mathcal{E}_h(\Gamma)} h_e \left\| (\boldsymbol{\sigma}_h \,+\, \boldsymbol{u}_h\otimes\boldsymbol{u}_h)^{\mathtt{d}}\, \boldsymbol{s} \,-\, \mu \frac{d\boldsymbol{u}_D}{d\boldsymbol{s}} \right\|_{0,e}^2 \Bigg\}^{1/2} \|\boldsymbol{\tau}\|_{\mathbf{div},\Omega} \,. \end{aligned} \tag{3.24}$$

Proof. Performing a local integration by parts on each element, and applying an integration–by–parts formula on the boundary (see [21, Lemma 3.8]), which makes use of the fact that $\nabla \boldsymbol{u}_D \in \mathbb{L}^2(\Gamma)$, we obtain

$$\begin{aligned} \mathcal{R}_2^{\mathbf{f}}(\underline{\mathbf{curl}}(\boldsymbol{\phi} - I_h\boldsymbol{\phi})) \,&=\, - \sum_{T\in\mathcal{T}_h} \int_T \big(\boldsymbol{\sigma}_h + \boldsymbol{u}_h\otimes\boldsymbol{u}_h\big)^{\mathtt{d}} : \underline{\mathbf{curl}}(\boldsymbol{\phi} - I_h\boldsymbol{\phi}) + \mu\langle\, \underline{\mathbf{curl}}(\boldsymbol{\phi} - I_h\boldsymbol{\phi})\, \boldsymbol{\nu}\,, \boldsymbol{u}_D \,\rangle_\Gamma \\ &= \sum_{T\in\mathcal{T}_h} \Big\{ - \int_T \mathrm{curl}\big((\boldsymbol{\sigma}_h \,+\, \boldsymbol{u}_h\otimes\boldsymbol{u}_h)^{\mathtt{d}}\big) \cdot (\boldsymbol{\phi} - I_h\boldsymbol{\phi}) \,+\, \sum_{e\subseteq\partial T} \int_e (\boldsymbol{\sigma}_h \,+\, \boldsymbol{u}_h\otimes\boldsymbol{u}_h)^{\mathtt{d}}\, \boldsymbol{s} \cdot (\boldsymbol{\phi} - I_h\boldsymbol{\phi}) \Big\} \\ &\quad - \mu \sum_{e\in\mathcal{E}_{h,T}(\Gamma)} \int_e \frac{d\boldsymbol{u}_D}{d\boldsymbol{s}} \cdot (\boldsymbol{\phi} - I_h\boldsymbol{\phi}) \\ &= - \sum_{T\in\mathcal{T}_h} \int_T \mathrm{curl}\big((\boldsymbol{\sigma}_h \,+\, \boldsymbol{u}_h\otimes\boldsymbol{u}_h)^{\mathtt{d}}\big) \cdot (\boldsymbol{\phi} - I_h\boldsymbol{\phi}) \,+ \sum_{e\in\mathcal{E}_h(\Omega)} \int_e [\![(\boldsymbol{\sigma}_h \,+\, \boldsymbol{u}_h\otimes\boldsymbol{u}_h)^{\mathtt{d}}\, \boldsymbol{s}]\!] \cdot (\boldsymbol{\phi} - I_h\boldsymbol{\phi}) \\ &\quad + \sum_{e\in\mathcal{E}_h(\Gamma)} \int_e \Big\{ (\boldsymbol{\sigma}_h \,+\, \boldsymbol{u}_h\otimes\boldsymbol{u}_h)^{\mathtt{d}}\, \boldsymbol{s} \,-\, \mu\, \frac{d\boldsymbol{u}_D}{d\boldsymbol{s}} \Big\} \cdot (\boldsymbol{\phi} - I_h\boldsymbol{\phi}) \\ &\leq \sum_{T\in\mathcal{T}_h} h_T \, \|\mathrm{curl}\big((\boldsymbol{\sigma}_h \,+\, \boldsymbol{u}_h\otimes\boldsymbol{u}_h)^{\mathtt{d}}\big)\|_{0,T} \, \|\boldsymbol{\phi}\|_{1,\Delta(T)} \,+\, \Bigg\{ \sum_{e\in\mathcal{E}_h(\Omega)} h_e^{1/2} \, \big\| [\![(\boldsymbol{\sigma}_h \,+\, \boldsymbol{u}_h\otimes\boldsymbol{u}_h)^{\mathtt{d}}\, \boldsymbol{s}]\!] \big\|_{0,e} \\ &\quad + \sum_{e\in\mathcal{E}_h(\Gamma)} h_e^{1/2} \left\| (\boldsymbol{\sigma}_h \,+\, \boldsymbol{u}_h\otimes\boldsymbol{u}_h)^{\mathtt{d}}\, \boldsymbol{s} \,-\, \mu\, \frac{d\boldsymbol{u}_D}{d\boldsymbol{s}} \right\|_{0,e} \Bigg\} \|\boldsymbol{\phi}\|_{1,\Delta(e)} \,, \end{aligned}$$

where the last statement follows by applying the Cauchy–Schwarz inequality, and using the local approximation properties of the Clément interpolant from Lemma 3.6. Finally, the estimate (3.24) is a consequence of the Cauchy-Schwarz inequality, the shape–regularity of the mesh and the fact that $\|\boldsymbol{\phi}\|_{1,\Omega} \leq C\|\boldsymbol{\tau}\|_{\mathbf{div},\Omega}$ in accordance to (3.17). □

We are in position to state the corresponding estimate for $\|\mathcal{R}^{\mathbf{f}}\|$.

Lemma 3.11 *There exists a positive constant $C > 0$, independent of h, such that*

$$\begin{aligned} \|\mathcal{R}^{\mathtt{f}}\| \,\le\, C \Bigg\{ \sum_{T\in\mathcal{T}_h} h_T^2 \,\|\mu\,\nabla\boldsymbol{u}_h \,-\, \boldsymbol{\sigma}_h^{\mathtt{d}} \,-\, (\boldsymbol{u}_h\otimes\boldsymbol{u}_h)^{\mathtt{d}}\|_{0,T}^2 \,+\, \kappa_2^2\,\|\mathbf{div}\,\boldsymbol{\sigma}_h \,+\, \varphi_h\,\boldsymbol{g}\|_{0,T}^2 \\ +\;\; h_T^2\,\|\mathrm{curl}\big((\boldsymbol{\sigma}_h \,+\, \boldsymbol{u}_h\otimes\boldsymbol{u}_h)^{\mathtt{d}}\big)\|_{0,T}^2 \,+ \sum_{e\in\mathcal{E}_h(\Omega)} h_e\,\|\,[\![(\boldsymbol{\sigma}_h \,+\, \boldsymbol{u}_h\otimes\boldsymbol{u}_h)^{\mathtt{d}}\,\boldsymbol{s})]\!]\|_{0,e}^2 \\ +\;\; \sum_{e\in\mathcal{E}_h(\Gamma)} h_e\Bigg\{\Big\|(\boldsymbol{\sigma}_h \,+\, \boldsymbol{u}_h\otimes\boldsymbol{u}_h)^{\mathtt{d}}\,\boldsymbol{s} \,-\, \mu\frac{d\boldsymbol{u}_D}{d\boldsymbol{s}}\Big\|_{0,e}^2 \,+\, \|\boldsymbol{u}_D - \boldsymbol{u}_h\|_{0,e}^2\Bigg\}\Bigg\}^{1/2}. \end{aligned} \tag{3.25}$$

Proof. It suffices to replace (3.22) into the first expression of (3.15), and then use there the estimates (3.23) and (3.24). We omit further details. □

At this point it is noteworthy to mention that differently from previous works (see, e.g. [2, 18, 16, 19, 20]), an integration–by–parts formula is employed in Lemma 3.8 to derive the residual term corresponding to the constitutive relation. The reason for this alternative procedure is elaborated next. Without integrating by parts, observe that the $\nabla\boldsymbol{z}$–dependent expression involved in (3.22) becomes

$$\begin{aligned} \mathcal{R}_1^{\mathtt{f}}(\nabla\boldsymbol{z} - \Pi_h^k(\nabla\boldsymbol{z})) \,=\, \mu\,\langle\,(\,\nabla\boldsymbol{z} \,-\, \Pi_h^k(\nabla\boldsymbol{z})\,)\,\boldsymbol{\nu}\,,\boldsymbol{u}_D\,\rangle_\Gamma \,-\, \mu\int_\Omega \boldsymbol{u}_h\cdot\mathbf{div}(\,\nabla\boldsymbol{z} \,-\, \Pi_h^k(\nabla\boldsymbol{z})\,) \\ -\;\; \int_\Omega \big(\boldsymbol{\sigma}_h \,+\, (\boldsymbol{u}_h\otimes\boldsymbol{u}_h)\big)^{\mathtt{d}} : (\,\nabla\boldsymbol{z} \,-\, \Pi_h^k(\nabla\boldsymbol{z})\,) \\ -\;\; \kappa_2\int_\Omega(\mathbf{div}(\boldsymbol{\sigma}_h) \,+\, \varphi_h\,\boldsymbol{g})\cdot\mathbf{div}(\,\nabla\boldsymbol{z} \,-\, \Pi_h^k(\nabla\boldsymbol{z})\,)\,. \end{aligned} \tag{3.26}$$

From the commuting property of the Raviart–Thomas spaces we have that $\mathbf{div}\circ\Pi_h^k = \mathcal{P}_h^k\circ\mathbf{div}$, where $\mathcal{P}_h^k$ is the orthogonal projection from $\mathbf{L}^2(\Omega)$ onto the polynomials of degree $\le k$ (see [14, Lemma 3.7] for instance), thus since $\mathbf{div}(\nabla\boldsymbol{z}) = \mathbf{div}(\boldsymbol{\tau}) \in \mathbf{L}^2(\Omega)$, we get on the one hand that

$$\int_\Omega \boldsymbol{u}_h\cdot\mathbf{div}(\,\nabla\boldsymbol{z} \,-\, \Pi_h^k(\nabla\boldsymbol{z})\,) \,=\, \sum_{T\in\mathcal{T}_h}\int_T \boldsymbol{u}_h\cdot(\,\mathbf{div}(\boldsymbol{\tau}) \,-\, \mathcal{P}_h^k(\mathbf{div}(\boldsymbol{\tau}))\,)\,, \tag{3.27}$$

and so the second term at the right–hand side of (3.26) would vanish if, and only if, $\boldsymbol{u}_h\big|_T \in \mathbf{P}_k(T)$ for all $T\in\mathcal{T}_h$. In turn, under this condition $\nabla\boldsymbol{u}_h\big|_T \in \mathbb{P}_{k-1}(T)$ for all $T\in\mathcal{T}_h$ and $\boldsymbol{u}_h\big|_e \in \mathbb{P}_k(e)$ on each $e\in\mathcal{E}_h$, and from the characterization of the Raviart–Thomas projector we also would have

$$\int_e \boldsymbol{u}_h : (\,\nabla\boldsymbol{z} \,-\, \Pi_h^k(\nabla\boldsymbol{z})\,) \,=\, 0 \quad \forall\, e\in\mathcal{E}_h \quad \text{and} \quad \int_T \nabla\boldsymbol{u}_h : (\,\nabla\boldsymbol{z} \,-\, \Pi_h^k(\nabla\boldsymbol{z})\,) \,=\, 0 \quad \forall\, T\in\mathcal{T}_h\,. \tag{3.28}$$

We then could suitably combine these latter expressions with the first and third terms at the right–hand side of (3.26) so as to get the residuals $\boldsymbol{u}_D - \boldsymbol{u}_h$ on Γ and $\mu\,\nabla\boldsymbol{u}_h - \boldsymbol{\sigma}_h^{\mathtt{d}} - (\boldsymbol{u}_h\otimes\boldsymbol{u}_h)^{\mathtt{d}}$ in Ω. However, recall that we approximate the velocity components by Lagrange elements of degree $k+1$ (cf. (2.12)) in order to achieve optimal–order a priori error estimates (cf. Section 2.3). Consequently, this leads us to preserve piecewise polynomials of degree $k+1$ for $\boldsymbol{u}$ and to increase the order for the Raviart–Thomas space instead from k to $k+1$ (cf. (2.12)), so that (3.27) and (3.28) hold, with Π_h^{k+1} and $\mathcal{P}_h^{k+1}$ in place of Π_h^k and $\mathcal{P}_h^k$, respectively. Nevertheless, Lemma 3.8 shows that this additional requirement is unnecessary.

We finally focus on estimating $\|\mathcal{R}^{\mathtt{h}}\|$.

Lemma 3.12 *There exists a positive constant $C > 0$, independent of h and $\widetilde{h}$, such that*

$$\|\mathcal{R}^{\mathtt{h}}\| \,\le\, C \left\{ \sum_{T\in\mathcal{T}_h} h_T^2 \|\mathrm{div}(\mathbb{K}\nabla\varphi_h) \,-\, \boldsymbol{u}_h\cdot\nabla\varphi_h\|_{0,T}^2 \right. \\ \left. +\, \sum_{e\in\mathcal{E}_h(\Omega)} h_e\, \| [\![\mathbb{K}\nabla\varphi_h\cdot\boldsymbol{\nu}]\!] \|_{0,e}^2 \,+\, \sum_{e\in\mathcal{E}_h(\Gamma)} h_e\, \|\lambda_{\widetilde{h}} \,+\, \mathbb{K}\nabla\varphi_h\cdot\boldsymbol{\nu}\|_{0,e}^2 \right\}^{1/2} \tag{3.29}$$

Proof. It basically follows by defining $\psi_h^{\mathcal{R}} = \mathcal{I}_h\psi$ in the second expression of (3.15), that is, as the respective Clemént interpolant of ψ in $\mathrm{H}^1(\Omega)$. Indeed, we first observe from (3.10) and the definitions of the forms involved, that

$$\mathcal{R}^{\mathtt{h}}(\psi-\psi_h^{\mathcal{R}}) \,=\, -\int_\Omega \big(\boldsymbol{u}_h\cdot\nabla\varphi_h\big)\,(\psi-\psi_h^{\mathcal{R}}) \,-\, \int_\Omega \mathbb{K}\nabla\varphi_h\cdot\nabla(\psi-\psi_h^{\mathcal{R}}) \,-\, \langle\lambda_{\widetilde{h}},\psi-\psi_h^{\mathcal{R}}\rangle_\Gamma\,,$$

which, after performing an element–wise integration by parts, becomes

$$\mathcal{R}^{\mathtt{h}}(\psi-\psi_h^{\mathcal{R}}) \,=\, \int_\Omega \big(\mathrm{div}(\mathbb{K}\nabla\varphi_h) \,-\, \boldsymbol{u}_h\cdot\nabla\varphi_h\big)\,(\psi-\psi_h^{\mathcal{R}}) \\ +\, \sum_{e\in\mathcal{E}_h(\Omega)} \int_e [\![\mathbb{K}\nabla\varphi_h\cdot\boldsymbol{\nu}]\!]\,(\psi-\psi_h^{\mathcal{R}}) \,-\, \sum_{e\in\mathcal{E}_h(\Gamma)} \int_e \big(\lambda_{\widetilde{h}} \,+\, \mathbb{K}\nabla\varphi_h\cdot\boldsymbol{\nu}\big)\,(\psi-\psi_h^{\mathcal{R}})\,.$$

Next, applying Cauchy-Schwarz's inequality and the approximation properties of the Clemént interpolator (cf. Lemma 3.6), we readily deduce the existence of a constant $C > 0$, such that

$$\big|\mathcal{R}^{\mathtt{h}}(\psi-\psi_h^{\mathcal{R}})\big| \,\le\, C \left\{ \sum_{T\in\mathcal{T}_h} h_T^2\, \|\mathrm{div}(\mathbb{K}\nabla\varphi_h) \,-\, \boldsymbol{u}_h\cdot\nabla\varphi_h\|_{0,T}^2 \right. \\ \left. +\, \sum_{e\in\mathcal{E}_h(\Omega)} h_e\, \| [\![\mathbb{K}\nabla\varphi_h\cdot\boldsymbol{\nu}]\!] \|_{0,e}^2 \,+\, \sum_{e\in\mathcal{E}_h(\Gamma)} h_e\, \|\lambda_{\widetilde{h}} \,+\, \mathbb{K}\nabla\varphi_h\cdot\boldsymbol{\nu}\|_{0,e}^2 \right\}^{1/2} \|\psi\|_{1,\Omega}\,,$$

which, replaced back into (3.15), leads to (3.29) and completes the proof. □

The reliability of the estimator $\boldsymbol{\theta}$ (cf. Lemma 3.1) essentially follows from Lemmas 3.4, 3.11 and 3.12. In this regard, we remark that the terms $h_T^2\,\|\mu\,\nabla\boldsymbol{u}_h \,-\, \boldsymbol{\sigma}_h^{\mathtt{d}} \,-\, (\boldsymbol{u}_h\otimes\boldsymbol{u}_h)^{\mathtt{d}}\|_{0,T}^2$ and $h_e\,\|\boldsymbol{u}_D \,-\, \boldsymbol{u}_h\|_{0,e}^2$ from the estimate (3.25) are not included in the definition of $\boldsymbol{\theta}_T^2$ since they are dominated by the expressions $\|\mu\,\nabla\boldsymbol{u}_h - \boldsymbol{\sigma}_h^{\mathtt{d}} - (\boldsymbol{u}_h\otimes\boldsymbol{u}_h)^{\mathtt{d}}\|_{0,T}$ and $\|\boldsymbol{u}_D - \boldsymbol{u}_h\|_{0,e}^2$, respectively, which already appear in the preliminary upper bound (3.4). Hence, an application of the Cauchy-Schwarz inequality immediately gives (3.3), with $C_{\mathrm{rel}} > 0$, independent of h and $\widetilde{h}$, according to the aforementioned lemmas.

3.3 Efficiency

The core of this section is to show the following result.

Theorem 3.13 *Let $(\boldsymbol{\sigma},\boldsymbol{u},\varphi,\lambda)$ and $(\boldsymbol{\sigma}_h,\boldsymbol{u}_h,\varphi_h,\lambda_{\widetilde{h}})$ be the unique solutions to problems (2.4) and (2.14), respectively, and assume that $\mathbb{K}$ and $\boldsymbol{u}_D$ are piecewise polynomials, $\boldsymbol{u}_D \in \mathbf{H}^1(\Gamma)$, the partition on Γ inherited from $\mathcal{T}_h$ is quasi-uniform, and each edge of $\mathcal{E}_h(\Gamma)$ is contained in one of the elements of the independent partition of Γ defining $\mathrm{H}_{\widetilde{h}}^{\lambda}$ (cf. (2.13)). Then, there exists a positive constant C_{eff}, depending on physical and stabilization parameters, but independent of h and $\widetilde{h}$, such that*

$$C_{\mathrm{eff}}\,\boldsymbol{\theta} \,\le\, \|(\boldsymbol{\sigma},\boldsymbol{u},\varphi,\lambda) \,-\, (\boldsymbol{\sigma}_h,\boldsymbol{u}_h,\varphi_h,\lambda_{\widetilde{h}})\|\,. \tag{3.30}$$

We first notice that if our problem were linear, establishing (3.30) would basically reduce to previously deriving upper bounds, depending on the local exact errors, for each one of the local terms defining $\boldsymbol{\theta}$ (cf. (3.1)–(3.2)) separately. In the present case, however, and because of the nonlinear character of our model, the above is only partially achieved (as we show later one), so that we mainly concentrate on obtaining the global efficiency estimates, as indeed is required by the inequality (3.30). Whenever some kind of local efficiency estimate is also possible, we make the corresponding remark below. In this regard, we mention in advance that only one of the local efficiency estimates to be specified in what follows is expressed in terms of the natural norms for the unknowns involved (cf. (3.37)). The rest of them arises by using local $\mathbf{L}^4$-norms of the error $\boldsymbol{u} - \boldsymbol{u}_h$ instead of the expected local $\mathbf{H}^1$-norm.

We begin with the corresponding estimates for

$$\|\varphi_h - \varphi_D\|_{1/2,\Gamma}\,, \quad \|\boldsymbol{u}_D - \boldsymbol{u}_h\|_{0,\Gamma}\,, \quad \|\mu\,\nabla\boldsymbol{u}_h - \boldsymbol{\sigma}_h^{\mathtt{d}} - (\boldsymbol{u}_h\otimes\boldsymbol{u}_h)^{\mathtt{d}}\|_{0,\Omega} \quad \text{and} \quad \|\mathbf{div}\,\boldsymbol{\sigma}_h + \varphi_h\,\boldsymbol{g}\|_{0,\Omega}\,.$$

Lemma 3.14 *There exists $C > 0$, independent of h and $\widetilde{h}$, such that*

$$\|\varphi_D - \varphi_h\|_{1/2,\Gamma}^2 + \|\boldsymbol{u}_D - \boldsymbol{u}_h\|_{0,\Gamma}^2 \,\le\, C\,\|(\boldsymbol{u},\varphi) - (\boldsymbol{u}_h,\varphi_h)\|^2\,, \tag{3.31}$$

and

$$\|\mu\,\nabla\boldsymbol{u}_h - \boldsymbol{\sigma}_h^{\mathtt{d}} - (\boldsymbol{u}_h\otimes\boldsymbol{u}_h)^{\mathtt{d}}\|_{0,\Omega}^2 + \|\mathbf{div}\,\boldsymbol{\sigma}_h + \varphi_h\,\boldsymbol{g}\|_{0,\Omega}^2 \,\le\, C\,\|(\boldsymbol{\sigma},\boldsymbol{u},\varphi) - (\boldsymbol{\sigma}_h,\boldsymbol{u}_h,\varphi_h)\|^2\,. \tag{3.32}$$

Proof. Since $\varphi|_\Gamma = \varphi_D$ and $\boldsymbol{u}|_\Gamma = \boldsymbol{u}_D$, the trace inequality immediately gives

$$\|\varphi_D - \varphi_h\|_{1/2,\Gamma}^2 \,=\, \|\varphi - \varphi_h\|_{1/2,\Gamma}^2 \,\le\, C\,\|\varphi - \varphi_h\|_{1,\Omega}^2\,,$$

and

$$\|\boldsymbol{u}_D - \boldsymbol{u}_h\|_{0,\Gamma}^2 \,=\, \|\boldsymbol{u} - \boldsymbol{u}_h\|_{0,\Gamma}^2 \,\le\, C\,\|\boldsymbol{u} - \boldsymbol{u}_h\|_{1,\Omega}^2\,,$$

which proves (3.31). In turn, using that $\mu\,\nabla\boldsymbol{u} - \boldsymbol{\sigma}^{\mathtt{d}} - (\boldsymbol{u}\otimes\boldsymbol{u})^{\mathtt{d}} = 0$ in Ω, we find by manipulating terms that

$$\begin{aligned}\|\mu\,\nabla\boldsymbol{u}_h - \boldsymbol{\sigma}_h^{\mathtt{d}} - (\boldsymbol{u}_h\otimes\boldsymbol{u}_h)^{\mathtt{d}}\|_{0,\Omega}^2 \,&=\, \|\mu\,\nabla(\boldsymbol{u}_h - \boldsymbol{u}) + (\boldsymbol{\sigma} - \boldsymbol{\sigma}_h)^{\mathtt{d}} + (\boldsymbol{u} + \boldsymbol{u}_h)^{\mathtt{d}}\otimes(\boldsymbol{u} - \boldsymbol{u}_h)^{\mathtt{d}}\|_{0,\Omega}^2 \\ &\le\, 4\Big\{\mu^2\,\|\boldsymbol{u} - \boldsymbol{u}_h\|_{1,\Omega}^2 + \|\boldsymbol{\sigma} - \boldsymbol{\sigma}_h\|_{\mathbf{div},\Omega}^2 + \|(\boldsymbol{u} + \boldsymbol{u}_h)\otimes(\boldsymbol{u} - \boldsymbol{u}_h)\|_{0,\Omega}^2\Big\}\,.\end{aligned} \tag{3.33}$$

Then, by applying Hölder's inequality, using the continuous injection $\mathbf{H}^1(\Omega) \hookrightarrow \mathbf{L}^4(\Omega)$, and bounding $\|\boldsymbol{u}\|_{1,\Omega}$ and $\|\boldsymbol{u}_h\|_{1,\Omega}$ by r (see at the end of Sections 2.2 and 2.3), we find

$$\|(\boldsymbol{u} + \boldsymbol{u}_h)\otimes(\boldsymbol{u} - \boldsymbol{u}_h)\|_{0,\Omega} \,\le\, \|\boldsymbol{u} + \boldsymbol{u}_h\|_{\mathbf{L}^4(\Omega)}\,\|\boldsymbol{u} - \boldsymbol{u}_h\|_{\mathbf{L}^4(\Omega)} \,\le\, C\,\|\boldsymbol{u} - \boldsymbol{u}_h\|_{1,\Omega}\,, \tag{3.34}$$

which, replaced back into (3.33), yields

$$\|\mu\,\nabla\boldsymbol{u}_h - \boldsymbol{\sigma}_h^{\mathtt{d}} - (\boldsymbol{u}_h\otimes\boldsymbol{u}_h)^{\mathtt{d}}\|_{0,\Omega}^2 \,\le\, C\Big\{\|\boldsymbol{\sigma} - \boldsymbol{\sigma}_h\|_{\mathbf{div},\Omega}^2 + \|\boldsymbol{u} - \boldsymbol{u}_h\|_{1,\Omega}^2\Big\}\,. \tag{3.35}$$

Likewise, since $\mathbf{div}\,\boldsymbol{\sigma} + \varphi\,\boldsymbol{g} = 0$ in Ω, we readily deduce that

$$\begin{aligned}\|\mathbf{div}\,\boldsymbol{\sigma}_h + \varphi_h\,\boldsymbol{g}\|_{0,\Omega}^2 \,&=\, \|\mathbf{div}\,(\boldsymbol{\sigma} - \boldsymbol{\sigma}_h) + (\varphi - \varphi_h)\,\boldsymbol{g}\|_{0,\Omega}^2 \\ &\le\, 2\big(1 + \|\boldsymbol{g}\|_{\infty,\Omega}^2\big)\Big\{\|\boldsymbol{\sigma} - \boldsymbol{\sigma}_h\|_{\mathbf{div},\Omega}^2 + \|\varphi - \varphi_h\|_{1,\Omega}^2\Big\}\,,\end{aligned} \tag{3.36}$$

and hence, the estimate (3.32) follows straightforwardly from (3.35) and (3.36). $\square$

At this point we observe that, proceeding as in (3.33) and (3.34) with $T \in \mathcal{T}_h$ instead of Ω, and bounding $\|\boldsymbol{u}\|_{\mathbf{L}^4(T)}$ and $\|\boldsymbol{u}_h\|_{\mathbf{L}^4(T)}$ by $\|\boldsymbol{u}\|_{\mathbf{L}^4(\Omega)}$ and $\|\boldsymbol{u}_h\|_{\mathbf{L}^4(\Omega)}$, respectively, and then both by a constant times r, we arrive at the local estimate

$$\|\mu\,\nabla \boldsymbol{u}_h - \boldsymbol{\sigma}_h^{\mathtt{d}} - (\boldsymbol{u}_h \otimes \boldsymbol{u}_h)^{\mathtt{d}}\|_{0,T}^2 \,\le\, C(\mu, r)\left\{\|\boldsymbol{u} - \boldsymbol{u}_h\|_{1,T}^2 \,+\, \|\boldsymbol{\sigma} - \boldsymbol{\sigma}_h\|_{\mathbf{div},T}^2 \,+\, \|\boldsymbol{u} - \boldsymbol{u}_h\|_{\mathbf{L}^4(T)}^2\right\},$$

where $C(\mu, r)$ is a positive constant depending on μ and r. In turn, we readily obtain, analogously to (3.36), but with $T \in \mathcal{T}_h$ instead of Ω, that

$$\|\mathbf{div}\,\boldsymbol{\sigma}_h \,+\, \varphi_h\,\boldsymbol{g}\|_{0,T}^2 \,\le\, 2\big(1 + \|\boldsymbol{g}\|_{\infty,T}^2\big)\left\{\|\boldsymbol{\sigma} - \boldsymbol{\sigma}_h\|_{\mathbf{div},T}^2 \,+\, \|\varphi - \varphi_h\|_{1,T}^2\right\}. \tag{3.37}$$

Throughout the rest of this section, for each $e \in \mathcal{E}_h(\Omega)$ we let ω_e be the union of the two elements of $\mathcal{T}_h$ having e as an edge. The following lemma deals with the remaining terms associated only to the fluid variables.

Lemma 3.15 *There exists $C > 0$, independent of h, such that*

$$\begin{aligned}\sum_{T\in\mathcal{T}_h} h_T^2\,\|\mathrm{curl}\big((\boldsymbol{\sigma}_h + \boldsymbol{u}_h \otimes \boldsymbol{u}_h)^{\mathtt{d}}\big)\|_{0,T}^2 \,+\, \sum_{e\in\mathcal{E}_h(\Omega)} h_e\,\|[\![(\boldsymbol{\sigma}_h + \boldsymbol{u}_h \otimes \boldsymbol{u}_h)^{\mathtt{d}}\,\boldsymbol{s}]\!]\|_{0,e}^2 \\ \le\quad C\,\|(\boldsymbol{\sigma}, \boldsymbol{u}) \,-\, (\boldsymbol{\sigma}_h, \boldsymbol{u}_h)\|^2\,.\end{aligned} \tag{3.38}$$

Additionally, if $\boldsymbol{u}_D$ is piecewise polynomial, there holds

$$\sum_{e\in\mathcal{E}_h(\Gamma)} h_e\,\left\|(\boldsymbol{\sigma}_h \,+\, \boldsymbol{u}_h \otimes \boldsymbol{u}_h)^{\mathtt{d}}\boldsymbol{s} \,-\, \mu\frac{d\boldsymbol{u}_D}{d\boldsymbol{s}}\right\|_{0,e}^2 \quad\le\quad C\,\|(\boldsymbol{\sigma}, \boldsymbol{u}) \,-\, (\boldsymbol{\sigma}_h, \boldsymbol{u}_h)\|^2\,. \tag{3.39}$$

Proof. From [19, Lemmas 4.9 and 4.10] we know that for each piecewise polynomial $\boldsymbol{\zeta}_h \in \mathbb{L}^2(\Omega)$, and for each $\boldsymbol{\zeta} \in \mathbb{L}^2(\Omega)$ with $\mathrm{curl}(\boldsymbol{\zeta}) = 0$ in Ω, there hold

$$\|\mathrm{curl}(\boldsymbol{\zeta}_h)\|_{0,T} \,\le\, C\,h_T^{-1}\,\|\boldsymbol{\zeta} - \boldsymbol{\zeta}_h\|_{0,T} \qquad \forall\, T \in \mathcal{T}_h$$

and

$$\|[\![\boldsymbol{\zeta}_h\,\boldsymbol{s}]\!]\|_{0,e} \,\le\, C\,h_e^{-1/2}\,\|\boldsymbol{\zeta} - \boldsymbol{\zeta}_h\|_{0,\omega_e} \qquad \forall\, e \in \mathcal{E}_h(\Omega)\,.$$

Hence, applying the foregoing inequalities with $\boldsymbol{\zeta}_h := \boldsymbol{\sigma}_h^{\mathtt{d}} + (\boldsymbol{u}_h \otimes \boldsymbol{u}_h)^{\mathtt{d}}$ and $\boldsymbol{\zeta} := \boldsymbol{\sigma}^{\mathtt{d}} + (\boldsymbol{u} \otimes \boldsymbol{u})^{\mathtt{d}} = \mu\nabla\boldsymbol{u}$ (whose curl clearly vanishes), we readily obtain

$$\begin{aligned}\|\mathrm{curl}\big((\boldsymbol{\sigma}_h + \boldsymbol{u}_h \otimes \boldsymbol{u}_h)^{\mathtt{d}}\big)\|_{0,T}^2 &\le C h_T^{-2}\,\|(\boldsymbol{\sigma} - \boldsymbol{\sigma}_h)^{\mathtt{d}} \,+\, (\boldsymbol{u} + \boldsymbol{u}_h)^{\mathtt{d}} \otimes (\boldsymbol{u} - \boldsymbol{u}_h)^{\mathtt{d}}\|_{0,T}^2 \\ &\le C h_T^{-2}\left\{\|\boldsymbol{\sigma} - \boldsymbol{\sigma}_h\|_{0,T}^2 \,+\, \|(\boldsymbol{u} + \boldsymbol{u}_h) \otimes (\boldsymbol{u} - \boldsymbol{u}_h)\|_{0,T}^2\right\},\end{aligned} \tag{3.40}$$

and also

$$\|[\![(\boldsymbol{\sigma}_h + \boldsymbol{u}_h \otimes \boldsymbol{u}_h)^{\mathtt{d}}\,\boldsymbol{s}]\!]\|_{0,e}^2 \le C h_e^{-1}\left\{\|\boldsymbol{\sigma} - \boldsymbol{\sigma}_h\|_{0,\omega_e}^2 \,+\, \|(\boldsymbol{u} + \boldsymbol{u}_h) \otimes (\boldsymbol{u} - \boldsymbol{u}_h)\|_{0,\omega_e}^2\right\}. \tag{3.41}$$

Then, adding on $T \in \mathcal{T}_h$ and $e \in \mathcal{E}_h(\Omega)$, respectively, we find

$$\begin{aligned}\sum_{T\in\mathcal{T}_h} h_T^2\,\|\mathrm{curl}\big((\boldsymbol{\sigma}_h + \boldsymbol{u}_h \otimes \boldsymbol{u}_h)^{\mathtt{d}}\big)\|_{0,T}^2 \,+\, \sum_{e\in\mathcal{E}_h(\Omega)} h_e\,\|[\![(\boldsymbol{\sigma}_h + \boldsymbol{u}_h \otimes \boldsymbol{u}_h)^{\mathtt{d}}\,\boldsymbol{s}]\!]\|_{0,e}^2 \\ \le\quad C\left\{\|\boldsymbol{\sigma} - \boldsymbol{\sigma}_h\|_{\mathrm{div},\Omega}^2 \,+\, \|(\boldsymbol{u} + \boldsymbol{u}_h) \otimes (\boldsymbol{u} - \boldsymbol{u}_h)\|_{0,\Omega}^2\right\},\end{aligned}$$

which, together with the estimate (3.34), yields (3.38). Likewise, (3.39) follows from a straightforward application of [19, Lemma 4.15] with $\boldsymbol{\sigma}_h^{\mathtt{d}} + (\boldsymbol{u}_h \otimes \boldsymbol{u}_h)^{\mathtt{d}}$ instead of $\dfrac{1}{2\mu}\boldsymbol{\sigma}_h^{\mathtt{d}}$, and using that $\dfrac{d\boldsymbol{u}_D}{d\boldsymbol{s}} = \nabla \boldsymbol{u}\, \boldsymbol{s} = \boldsymbol{\sigma}_h^{\mathtt{d}} + (\boldsymbol{u}_h \otimes \boldsymbol{u}_h)^{\mathtt{d}}\, \boldsymbol{s}$ on Γ, which gives for each e in $\mathcal{E}_h(\Gamma)$

$$\left\|(\boldsymbol{\sigma}_h + \boldsymbol{u}_h \otimes \boldsymbol{u}_h)^{\mathtt{d}}\boldsymbol{s} - \mu\frac{d\boldsymbol{u}_D}{d\boldsymbol{s}}\right\|_{0,e}^2 \leq C\, h_e^{-1} \left\|(\boldsymbol{\sigma} + \boldsymbol{u} \otimes \boldsymbol{u})^{\mathtt{d}} - (\boldsymbol{\sigma}_h + \boldsymbol{u}_h \otimes \boldsymbol{u}_h)^{\mathtt{d}}\right\|_{0,T_e}^2, \tag{3.42}$$

where T_e is the triangle in $\mathcal{T}_h$ having e as an edge. The rest of the proof is reduced simply to add on $e \in \mathcal{E}_h(\Gamma)$, to manipulate terms, and to apply again the bound (3.34). □

We point out here that, for simplicity, the derivation of (3.39) in Lemma 3.15 has assumed $\boldsymbol{u}_D$ to be piecewise polynomial. If this is not the case, but $\boldsymbol{u}_D$ is sufficiently smooth, then we still could derive an analogous estimate by using a suitable polynomial approximation of this datum, so that as a result of it, higher order terms would appear.

Furthermore, from (3.40), (3.41), and (3.42), together with the local version of the first inequality in (3.34), using again that $\|\boldsymbol{u}\|_{\mathbf{L}^4(T)}$ and $\|\boldsymbol{u}_h\|_{\mathbf{L}^4(T)}$ are dominated by a constant times r, we deduce the local efficiency estimates

$$h_T^2\, \|\mathrm{curl}\big((\boldsymbol{\sigma}_h + \boldsymbol{u}_h \otimes \boldsymbol{u}_h)^{\mathtt{d}}\big)\|_{0,T}^2 \leq C(r)\left\{\|\boldsymbol{\sigma} - \boldsymbol{\sigma}_h\|_{0,T}^2 + \|\boldsymbol{u} - \boldsymbol{u}_h\|_{\mathbf{L}^4(T)}^2\right\} \qquad \forall\, T \in \mathcal{T}_h\,,$$

$$h_e\, \|[\![(\boldsymbol{\sigma}_h + \boldsymbol{u}_h \otimes \boldsymbol{u}_h)^{\mathtt{d}}\, \boldsymbol{s}]\!]\|_{0,e}^2 \leq C(r)\left\{\|\boldsymbol{\sigma} - \boldsymbol{\sigma}_h\|_{0,\omega_e}^2 + \|\boldsymbol{u} - \boldsymbol{u}_h\|_{\mathbf{L}^4(\omega_e)}^2\right\} \qquad \forall\, e \in \mathcal{E}_h(\Omega)\,,$$

and

$$h_e \left\|(\boldsymbol{\sigma}_h + \boldsymbol{u}_h \otimes \boldsymbol{u}_h)^{\mathtt{d}}\boldsymbol{s} - \mu\frac{d\boldsymbol{u}_D}{d\boldsymbol{s}}\right\|_{0,e}^2 \leq C(r)\left\{\|\boldsymbol{\sigma} - \boldsymbol{\sigma}_h\|_{0,T_e}^2 + \|\boldsymbol{u} - \boldsymbol{u}_h\|_{\mathbf{L}^4(T_e)}^2\right\} \qquad \forall\, e \in \mathcal{E}_h(\Gamma)\,,$$

with a constant $C(r)$ depending on r.

Before proceeding with the residual terms related to the heat equation, we first recall the usual triangle–bubble and edge–bubble functions ψ_T and ψ_e defined for each $T \in \mathcal{T}_h$ and $e \subseteq \partial T$, respectively, satisfying the properties:

(b.1) $\psi_T \in \mathrm{P}_3(T)\,,\ \mathtt{supp}(\psi_T) \subseteq T\,,\ \psi_T = 0$ on ∂T, and $0 \leq \psi_T \leq 1$.

(b.2) $\psi_e \in \mathrm{P}_2(T)\,,\ \mathtt{supp}(\psi_e) \subseteq \omega_e\,,\ \psi_e = 0$ on $\partial T \setminus e$, and $0 \leq \psi_e \leq 1$.

We then recall the following useful and standard results.

Lemma 3.16 *Given an integer $k \geq 0$, for each $T \in \mathcal{T}_h$ and $e \subseteq \partial T$, there exists an extension operator $L : \mathrm{C}(e) \to \mathrm{C}(T)$ such that $L(p) \in \mathrm{P}_k(T)$ for all $p \in \mathrm{P}_k(e)$. Moreover, there exist positive constants c_1, c_2 and c_3, depending only on k and the shape regularity of the triangulation (minimum angle condition), such that*

$$\|q\|_{0,T}^2 \leq c_1 \|\psi_T^{1/2}\, q\|_{0,T}^2 \quad \forall\, q \in \mathrm{P}_k(T) \tag{3.43a}$$

$$\|p\|_{0,e}^2 \leq c_2 \|\psi_e^{1/2}\, p\|_{0,e}^2 \quad \forall\, p \in \mathrm{P}_k(e) \tag{3.43b}$$

$$\|\psi_e\, L(p)\|_{0,T}^2 \leq \|\psi_e^{1/2}\, L(p)\|_{0,T}^2 \leq c_3\, h_e \|p\|_{0,e}^2 \quad \forall\, p \in \mathrm{P}_k(e) \tag{3.43c}$$

Lemma 3.17 *Let $k, l, m \in \mathrm{N} \cup \{0\}$, such that $l \le m$. Then, there exists $c > 0$, depending only on k, l and m and the shape regularity of the triangulation, such that for each $T \in \mathcal{T}_h$ there holds*

$$|q|_{m,T} \,\le\, c h_T^{l-m} |q|_{l,T} \quad \forall\, q \in \mathrm{P}_k(T)$$

We are now ready to derive the final estimates required for stating the efficiency of $\boldsymbol{\theta}$.

Lemma 3.18 *Assume that $\mathbb{K}$ is piecewise polynomial. Then there exists $C > 0$, independent of h and $\widetilde{h}$, such that*

$$\sum_{T\in\mathcal{T}_h} h_T^2 \,\|\, \mathrm{div}(\mathbb{K}\nabla\varphi_h) \,-\, \boldsymbol{u}_h\cdot\nabla\varphi_h \,\|_{0,T}^2 \,\le\, C\,\|(\boldsymbol{u},\varphi) \,-\, (\boldsymbol{u}_h,\varphi_h)\|^2\,. \tag{3.44}$$

Proof. Given $T \in \mathcal{T}_h$, we define the local polynomial

$$\chi_T \,:=\, \mathrm{div}(\mathbb{K}\nabla\varphi_h) \,-\, \boldsymbol{u}_h\cdot\nabla\varphi_h\big|_T\,.$$

Thus, applying the upper bound (3.43a), and then integrating by parts, using that $\mathtt{supp}(\psi_T) \subseteq T$ according to **(b.1)** above, we find that

$$\begin{aligned}
\|\chi_T\|_{0,T}^2 \,&\le\, c_1\,\|\psi_T^{1/2}\,\chi_T\|_{0,T}^2 \,=\, c_1 \int_T \big(\,\mathrm{div}(\mathbb{K}\nabla\varphi_h) \,-\, \boldsymbol{u}_h\cdot\nabla\varphi_h\,\big)\,\psi_T\,\chi_T \\
&=\, c_1\Big\{\,-\int_T \mathbb{K}\nabla\varphi_h\cdot\nabla(\psi_T\,\chi_T) \,-\, \int_T \big(\boldsymbol{u}_h\cdot\nabla\varphi_h\big)\,\psi_T\,\chi_T\,\Big\}\,.
\end{aligned} \tag{3.45}$$

Next, from the second equation of (2.4) we have that $\mathbf{a}(\varphi,\,\psi) + \mathbf{b}(\psi,\lambda) \,=\, F_{\boldsymbol{u},\varphi}(\psi)$ for all $\psi \in \mathrm{H}^1(\Omega)$, so that taking in particular $\psi = \psi_T\,\chi_T$, we get

$$\int_T \mathbb{K}\nabla\varphi\cdot\nabla(\psi_T\,\chi_T) \,+\, \int_T \big(\boldsymbol{u}\cdot\nabla\varphi\big)\,\psi_T\,\chi_T \,=\, 0\,, \tag{3.46}$$

which, combined with (3.45), and applying Hölder's inequality, yields

$$\begin{aligned}
\|\chi_T\|_{0,T}^2 \,&\le\, c_1\bigg\{\,\int_T \mathbb{K}\nabla(\varphi-\varphi_h)\cdot\nabla(\psi_T\,\chi_T) \\
&+\, \int_T \Big\{\,(\boldsymbol{u}-\boldsymbol{u}_h)\cdot\nabla\varphi \,+\, \boldsymbol{u}_h\cdot\nabla(\varphi-\varphi_h)\,\Big\}\,\psi_T\,\chi_T\bigg\} \\
&\le\quad c_1\Big\{\,\|\mathbb{K}\|_{\infty,T}\,|\varphi-\varphi_h|_{1,T}\,|\psi_T\,\chi_T|_{1,T} \\
&+\quad \Big(\,\|\boldsymbol{u}-\boldsymbol{u}_h\|_{\mathbf{L}^4(T)}\,\|\nabla\varphi\|_{0,T} \,+\, \|\boldsymbol{u}_h\|_{\mathbf{L}^4(T)}\,\|\nabla(\varphi-\varphi_h)\|_{0,T}\,\Big)\,\|\psi_T\,\chi_T\|_{\mathrm{L}^4(T)}\Big\} \\
&\le\quad c_1\,C\Big\{\,\|\mathbb{K}\|_{\infty,T}\,|\varphi-\varphi_h|_{1,T} \\
&+\quad \|\boldsymbol{u}-\boldsymbol{u}_h\|_{\mathbf{L}^4(T)}\,|\varphi|_{1,T} \,+\, \|\boldsymbol{u}_h\|_{\mathbf{L}^4(T)}\,|\varphi-\varphi_h|_{1,T}\,\Big\}\,|\psi_T\,\chi_T|_{1,T}\,,
\end{aligned} \tag{3.47}$$

where the last inequality makes use of the estimate

$$\|\psi_T\,\chi_T\|_{\mathrm{L}^4(T)} \,\le\, \|\psi_T\,\chi_T\|_{\mathrm{L}^4(\Omega)} \,\le\, C\,\|\psi_T\,\chi_T\|_{1,\Omega} \,\le\, C\,|\psi_T\,\chi_T|_{1,\Omega} \,=\, C|\psi_T\,\chi_T|_{1,T}\,, \tag{3.48}$$

which follows from the continuous injection $\mathrm{H}^1(\Omega) \hookrightarrow \mathrm{L}^4(\Omega)$, the fact that $\mathtt{supp}(\psi_T) \subseteq T$, and the usual Poincaré inequality in Ω. Next, using the inverse inequality provided by Lemma 3.17 with $m = 1$ and $l = 0$, we have that

$$|\psi_T\,\chi_T|_{1,T} \,\leq\, c\,h_T^{-1}\,\|\psi_T\,\chi_T\|_{0,T} \,\leq\, c\,h_T^{-1}\,\|\chi_T\|_{0,T}\,,$$

which, replaced back in (3.47), gives

$$\|\chi_T\|_{0,T}^2 \,\leq\, C\,h_T^{-1}\,\Big\{\Big(\|\mathbb{K}\|_{\infty,T} \,+\, \|\boldsymbol{u}_h\|_{\mathbf{L}^4(T)}\Big)\,|\varphi-\varphi_h|_{1,T} \,+\, |\varphi|_{1,T}\,\|\boldsymbol{u}-\boldsymbol{u}_h\|_{\mathbf{L}^4(T)}\Big\}\,\|\chi_T\|_{0,T}$$

and therefore

$$h_T^2\,\|\chi_T\|_{0,T}^2 \,\leq\, C\,\Big\{\Big(\|\mathbb{K}\|_{\infty,T} \,+\, \|\boldsymbol{u}_h\|_{\mathbf{L}^4(T)}\Big)^2\,|\varphi-\varphi_h|_{1,T}^2 \,+\, |\varphi|_{1,T}^2\,\|\boldsymbol{u}-\boldsymbol{u}_h\|_{\mathbf{L}^4(T)}^2\Big\}\,. \tag{3.49}$$

Now, bounding $\|\mathbb{K}\|_{\infty,T}$ and $\|\boldsymbol{u}_h\|_{\mathbf{L}^4(T)}$ by $\|\mathbb{K}\|_{\infty,\Omega}$ and $\|\boldsymbol{u}_h\|_{\mathbf{L}^4(\Omega)}$, respectively, using the continuous injection $\mathrm{H}^1(\Omega) \hookrightarrow \mathrm{L}^4(\Omega)$, and recalling from the discrete analysis that $\|\boldsymbol{u}_h\|_{1,\Omega} \,\leq\, r$, we deduce that

$$\sum_{T\in\mathcal{T}_h}\Big(\|\mathbb{K}\|_{\infty,T} \,+\, \|\boldsymbol{u}_h\|_{\mathbf{L}^4(T)}\Big)^2\,|\varphi-\varphi_h|_{1,T}^2 \,\leq\, C\,\big(\|\mathbb{K}\|_{\infty,\Omega}^2 \,+\, r^2\big)\,|\varphi-\varphi_h|_{1,\Omega}^2\,. \tag{3.50}$$

In turn, bounding one factor $|\varphi|_{1,T}$ by $|\varphi|_{1,\Omega}$, applying the Cauchy-Schwarz inequality to the remaining two factors, employing again the aforementioned continuous injection, and recalling from the continuous analysis that $\|\varphi\|_{1,\Omega} \,\leq\, r$, we obtain

$$\begin{aligned}\sum_{T\in\mathcal{T}_h}|\varphi|_{1,T}^2\,\|\boldsymbol{u}-\boldsymbol{u}_h\|_{\mathbf{L}^4(T)}^2 \,&\leq\, |\varphi|_{1,\Omega}\,\Bigg\{\sum_{T\in\mathcal{T}_h}|\varphi|_{1,T}^2\Bigg\}^{1/2}\,\Bigg\{\sum_{T\in\mathcal{T}_h}\|\boldsymbol{u}-\boldsymbol{u}_h\|_{\mathbf{L}^4(T)}^4\Bigg\}^{1/2}\\ &=\, |\varphi|_{1,\Omega}^2\,\|\boldsymbol{u}-\boldsymbol{u}_h\|_{\mathbf{L}^4(\Omega)}^2 \,\leq\, C\,r^2\,\|\boldsymbol{u}-\boldsymbol{u}_h\|_{1,\Omega}^2\,.\end{aligned} \tag{3.51}$$

In this way, bearing in mind the early definition of χ_T, summing up over all $T \in \mathcal{T}_h$ in (3.49), and utilizing the estimates (3.50) and (3.51), we arrive at (3.44), which ends the proof. □

It is straightforward to see from (3.49) that the local efficiency estimate associated to the previous lemma becomes

$$h_T^2\,\|\mathrm{div}(\mathbb{K}\nabla\varphi_h) \,-\, \boldsymbol{u}_h\cdot\nabla\varphi_h\|_{0,T}^2 \,\leq\, C(r,\mathbb{K})\,\Big\{|\varphi-\varphi_h|_{1,T}^2 \,+\, \|\boldsymbol{u}-\boldsymbol{u}_h\|_{\mathbf{L}^4(T)}^2\Big\}\,, \tag{3.52}$$

where $C(r,\mathbb{K})$ is a positive constant depending on r and $\|\mathbb{K}\|_{\infty,\Omega}$.

Lemma 3.19 *Assume that $\mathbb{K}$ is piecewise polynomial. Then there exists $C > 0$, independent of h and $\widetilde{h}$, such that*

$$\sum_{e\in\mathcal{E}_h(\Omega)} h_e\,\|\,[\![\mathbb{K}\nabla\varphi_h\cdot\boldsymbol{\nu}]\!]\,\|_{0,e}^2 \,\leq\, C\,\|(\boldsymbol{u},\varphi) \,-\, (\boldsymbol{u}_h,\varphi_h)\|^2\,. \tag{3.53}$$

Proof. Given $e \in \mathcal{E}_h(\Omega)$, we first define the polynomial

$$\chi_e \,:=\, [\![\mathbb{K}\nabla\varphi_h\cdot\boldsymbol{\nu}]\!] \quad \text{on} \quad e\,,$$

and then apply (3.43b) and integrate by parts, to find

$$
\begin{aligned}
\|\chi_e\|_{0,e}^2 \,&\le\, c_2\,\|\psi_e^{1/2}\,\chi_e\|_{0,e}^2 \,=\, c_2 \int_e [\![\mathbb{K}\nabla\varphi_h\cdot\boldsymbol{\nu}]\!]\,\psi_e\chi_e \\
&=\quad c_2 \int_e [\![\mathbb{K}\nabla\varphi_h\cdot\boldsymbol{\nu}]\!]\,\psi_e L(\chi_e) \,=\, c_2 \sum_{T\subseteq\omega_e} \int_{\partial T} \mathbb{K}\nabla\varphi_h\cdot\boldsymbol{\nu}\,\psi_e L(\chi_e) \\
&= c_2 \sum_{T\subseteq\omega_e} \left\{ \int_T \mathbb{K}\nabla\varphi_h\cdot\nabla(\psi_e L(\chi_e)) \,+\, \int_T \operatorname{div}(\mathbb{K}\nabla\varphi_h)\psi_e L(\chi_e) \right\}.
\end{aligned}
\tag{3.54}
$$

Now, because of the same arguments yielding (3.46), but using $\psi_e L(\chi_e)$ and ω_e in place of $\psi_T\,\chi_T$ and $T\in\mathcal{T}_h$, respectively, we obtain

$$
\sum_{T\,\subseteq\,\omega_e} \left\{ \int_T \mathbb{K}\nabla\varphi\cdot\nabla(\psi_e\,L(\chi_e)) \,+\, \int_T \big(\boldsymbol{u}\cdot\nabla\varphi\big)\,\psi_e\,L(\chi_e) \right\} \,=\, 0\,. \tag{3.55}
$$

Thus, replacing $\boldsymbol{u}\cdot\nabla\varphi$ in the foregoing null equation by the identity

$$
\boldsymbol{u}\cdot\nabla\varphi \,=\, \boldsymbol{u}_h\cdot\nabla\varphi_h \,-\, (\boldsymbol{u}_h-\boldsymbol{u})\cdot\nabla\varphi \,-\, \boldsymbol{u}_h\cdot\nabla(\varphi_h-\varphi)\,, \tag{3.56}
$$

and incorporating the resulting expression into (3.54) , we arrive at

$$
\begin{aligned}
\|\chi_e\|_{0,e}^2 \,\le\, c_2 &\sum_{T\subseteq\omega_e} \left\{ \int_T \mathbb{K}\nabla(\varphi_h-\varphi)\cdot\nabla(\psi_e L(\chi_e)) \right.\\
&+\quad \int_T \Big\{(\boldsymbol{u}_h-\boldsymbol{u})\cdot\nabla\varphi \,+\, \boldsymbol{u}_h\cdot\nabla(\varphi_h-\varphi)\Big\}\,\psi_e L(\chi_e) \\
&+\quad \left.\int_T \Big\{\operatorname{div}(\mathbb{K}\nabla\varphi_h) \,-\, \boldsymbol{u}_h\cdot\nabla\varphi_h\Big\}\,\psi_e L(\chi_e)\right\}.
\end{aligned}
\tag{3.57}
$$

Next, similarly as for the derivation of (3.47), straightforward applications of the Cauchy-Schwarz and Hölder inequalities yield

$$
\begin{aligned}
\|\chi_e\|_{0,e}^2 \,\le\, c_2 &\sum_{T\subseteq\omega_e} \left\{ \|\mathbb{K}\|_{\infty,T}\,|\varphi-\varphi_h|_{1,T}\,|\psi_e L(\chi_e)|_{1,T} \right.\\
+\quad &\Big(\|\boldsymbol{u}-\boldsymbol{u}_h\|_{\mathbf{L}^4(T)}\,|\varphi|_{1,T} \,+\, \|\boldsymbol{u}_h\|_{\mathbf{L}^4(T)}\,|\varphi-\varphi_h|_{1,T}\Big)\,\|\psi_e L(\chi_e)\|_{\mathrm{L}^4(T)} \\
+\quad &\left.\|\operatorname{div}(\mathbb{K}\nabla\varphi_h) \,-\, \boldsymbol{u}_h\cdot\nabla\varphi_h\|_{0,T}\,\|\psi_e L(\chi_e)\|_{0,T}\right\}.
\end{aligned}
$$

In this way, utilizing the inverse estimate from Lemma 3.17, the upper bound (3.43c), and the fact that $\|\psi_e L(\chi_e)\|_{\mathrm{L}^4(T)} \,\le\, c\,|\psi_e L(\chi_e)|_{1,\omega_e}$, whose proof follows similarly to (3.48), we deduce

$$
\begin{aligned}
\|\chi_e\|_{0,e}^2 \,\le\, C &\sum_{T\subseteq\omega_e} \left\{ h_T^{-1}\,\|\mathbb{K}\|_{\infty,T}\,|\varphi-\varphi_h|_{1,T} \right.\\
+\quad &h_T^{-1}\,\Big(\,|\varphi|_{1,T}\,\|\boldsymbol{u}-\boldsymbol{u}_h\|_{\mathbf{L}^4(T)} \,+\, \|\boldsymbol{u}_h\|_{\mathbf{L}^4(T)}\,|\varphi-\varphi_h|_{1,T}\Big) \\
+\quad &\left.\|\operatorname{div}(\mathbb{K}\nabla\varphi_h) \,-\, \boldsymbol{u}_h\cdot\nabla\varphi_h\|_{0,T}\right\}\,h_e^{1/2}\,\|\chi_e\|_{0,e}\,,
\end{aligned}
\tag{3.58}
$$

from which, simple algebraic manipulations give

$$
\begin{aligned}
h_e \,\|\chi_e\|_{0,e}^2 \,\le\, C \sum_{T\subseteq\omega_e} \Big\{ & \big(\|\mathbb{K}\|_{\infty,T} \,+\, \|\boldsymbol{u}_h\|_{\mathbf{L}^4(T)}\big)^2\, |\varphi-\varphi_h|_{1,T}^2 \,+\, |\varphi|_{1,T}^2\, \|\boldsymbol{u}-\boldsymbol{u}_h\|_{\mathbf{L}^4(T)}^2 \\
& + \; h_T^2\, \|\mathrm{div}(\mathbb{K}\nabla\varphi_h) \,-\, \boldsymbol{u}_h\cdot\nabla\varphi_h\|_{0,T}^2 \Big\}.
\end{aligned}
\tag{3.59}
$$

Finally, summing up over all $e \in \mathcal{E}_h(\Omega)$ in (3.59), noting that

$$
\sum_{e\in\mathcal{E}_h(\Omega)} \sum_{T\subseteq\omega_e} \,\le\, 3 \sum_{T\in\mathcal{T}_h} ,
$$

and using the previous estimates (3.50), (3.51), and (3.44), we obtain (3.53), which completes the proof. □

Here we observe from (3.52) and (3.59) that the local efficiency estimate associated to Lemma 3.19 is given by

$$
h_e \,\|\, [\![\mathbb{K}\nabla\varphi_h\cdot\boldsymbol{\nu}]\!] \,\|_{0,e}^2 \,\le\, \widetilde{C}(r,\mathbb{K}) \sum_{T\subseteq\omega_e} \Big\{ |\varphi-\varphi_h|_{1,T}^2 \,+\, \|\boldsymbol{u}-\boldsymbol{u}_h\|_{\mathbf{L}^4(T)}^2 \Big\} \qquad \forall\, e\in\mathcal{E}_h(\Omega)
$$

where $\widetilde{C}(r,\mathbb{K})$ is another positive constant depending on r and $\|\mathbb{K}\|_{\infty,\Omega}$.

The remaining term defining $\boldsymbol{\theta}$ and involving the Lagrange multiplier is addressed next.

Lemma 3.20 *Assume for simplicity that $\mathbb{K}$ is piecewise polynomial, that the partition on Γ inherited from $\mathcal{T}_h$ is quasi-uniform, and that each edge of $\mathcal{E}_h(\Gamma)$ is contained in one of the elements of the independent partition of Γ defining $\mathrm{H}_{\widetilde{h}}^{\lambda}$ (cf. (2.13)). Then, there exists $C>0$, independent of h and $\widetilde{h}$, such that*

$$
\sum_{e\in\mathcal{E}_h(\Gamma)} h_e\,\|\lambda_{\widetilde{h}} + \mathbb{K}\nabla\varphi_h\cdot\boldsymbol{\nu}\|_{0,e}^2 \,\le\, C\,\|(\boldsymbol{u},\varphi,\lambda) \,-\, (\boldsymbol{u}_h,\varphi_h,\lambda_{\widetilde{h}})\|^2 .
$$

Proof. We begin by defining, for each $e\in\mathcal{E}_h(\Gamma)$, the polynomial $\chi_e := \lambda_{\widetilde{h}} + \mathbb{K}\nabla\varphi_h\cdot\boldsymbol{\nu}$ on e. Note here that the assumption on the edges of $\mathcal{E}_h(\Gamma)$ insures that χ_e is indeed a polynomial (and not a piecewise polynomial). Then, applying (3.43b), denoting by T_e the element of $\mathcal{T}_h$ whose boundary edge is e, recalling that the edge-bubble function ψ_e vanishes on $\partial T_e\setminus e$, and integrating by parts, we obtain

$$
\begin{aligned}
\|\chi_e\|_{0,e}^2 \,\le\, c_2\,\|\psi_e^{1/2}\,\chi_e\|_{0,e}^2 \,&=\, c_2\int_e (\lambda_{\widetilde{h}} \,+\, \mathbb{K}\nabla\varphi_h\cdot\boldsymbol{\nu})\,\psi_e\chi_e \\
&=\, c_2\Big\{\langle\lambda_{\widetilde{h}},\psi_e\,\chi_e\rangle_e \,+\, \int_{\partial T_e}\mathbb{K}\nabla\varphi_h\cdot\boldsymbol{\nu}\,\psi_e L(\chi_e)\Big\} \\
&=\, c_2\Big\{\langle\lambda_{\widetilde{h}},\psi_e\,\chi_e\rangle_e \,+\, \int_{T_e}\mathbb{K}\nabla\varphi_h\cdot\nabla(\psi_e L(\chi_e)) \,+\, \int_{T_e}\mathrm{div}(\mathbb{K}\nabla\varphi_h)\psi_e L(\chi_e)\Big\},
\end{aligned}
\tag{3.60}
$$

where $\langle\cdot,\cdot\rangle_e$ stands for the duality pairing between $\mathrm{H}_{00}^{-1/2}(e)$ and $\mathrm{H}_{00}^{1/2}(e)$. Next, similarly as in the proofs of the two previous lemmas (cf. (3.46) and (3.55)), we deduce from the second equation of the continuous formulation (2.4), by taking now $\psi=\psi_e\,L(\chi_e)$, that

$$
\int_{T_e}\mathbb{K}\nabla\varphi\cdot\nabla(\psi_e\,L(\chi_e)) \,+\, \langle\lambda,\psi_e\,\chi_e\rangle_e \,+\, \int_{T_e}\big(\boldsymbol{u}\cdot\nabla\varphi\big)\,\psi_e L(\chi_e) \,=\, 0\,,
$$

which, subtracted from the right hand side of (3.60), and using again the identity (3.56) (as we did for obtaining (3.57)), yields

$$
\begin{aligned}
\|\chi_e\|_{0,e}^2 \,\le\, c_2 \Big\{ &\langle \lambda_{\widetilde{h}} - \lambda, \psi_e\, \chi_e\rangle_e \,+\, \int_{T_e} \mathbb{K}\nabla\big(\varphi_h - \varphi\big)\cdot\nabla(\psi_e L(\chi_e)) \\
+ \quad &\int_{T_e} \Big\{ (\boldsymbol{u}_h - \boldsymbol{u})\cdot\nabla\varphi \,+\, \boldsymbol{u}_h\cdot\nabla(\varphi_h - \varphi) \Big\}\,\psi_e L(\chi_e) \\
+ \quad &\int_{T_e} \Big\{ \mathrm{div}(\mathbb{K}\nabla\varphi_h) \,-\, \boldsymbol{u}_h\cdot\nabla\varphi_h \Big\}\,\psi_e L(\chi_e) \Big\}\,.
\end{aligned}
\tag{3.61}
$$

In this way, since the three integrals on the right hand side of the foregoing equation look exactly as those on the right hand side of (3.57), the rest of the analysis aiming to obtain its corresponding efficiency estimate follows verbatim as we did for (3.57), thus yielding a bound depending on the error $\|(\boldsymbol{u},\varphi) - (\boldsymbol{u}_h,\varphi_h)\|$, in accordance to (3.58) and (3.53). Hence, it only remains now to get the respective upper bound for the expression defined in terms of $\langle \lambda_{\widetilde{h}} - \lambda, \psi_e\, \chi_e\rangle_e$. To this end, and proceeding as in the proof of [13, Lemma 5.7], we first notice that

$$
\sum_{e\in\mathcal{E}_h(\Gamma)} h_e\,\langle \lambda_{\widetilde{h}} - \lambda, \psi_e\,\chi_e\rangle_e \,=\, \langle \lambda_{\widetilde{h}} - \lambda, \widetilde{\psi}\rangle_\Gamma\,,
$$

where $\widetilde{\psi} \in \mathrm{H}^{1/2}(\Gamma)$ is the piecewise polynomial defined as $\widetilde{\psi}|_e \,=\, h_e\,\psi_e\,\chi_e$ for each $e \in \mathcal{E}_h(\Gamma)$. Therefore, applying an inverse inequality to $\widetilde{\psi}$ (which makes use of the quasi-uniformity assumption on Γ), and noting that

$$
\|\widetilde{\psi}\|_{0,\Gamma} \,\le\, h^{1/2} \left\{ \sum_{e\in\mathcal{E}_h(\Gamma)} h_e\,\|\chi_e\|_{0,e}^2 \right\}^{1/2},
$$

we deduce that

$$
\begin{aligned}
\left| \sum_{e\in\mathcal{E}_h(\Gamma)} h_e\,\langle \lambda_{\widetilde{h}} - \lambda, \psi_e\,\chi_e\rangle_e \right| \,&\le\, \|\lambda - \lambda_{\widetilde{h}}\|_{-1/2,\Gamma}\,\|\widetilde{\psi}\|_{1/2,\Gamma} \,\le\, c\,h^{-1/2}\,\|\lambda - \lambda_{\widetilde{h}}\|_{-1/2,\Gamma}\,\|\widetilde{\psi}\|_{0,\Gamma} \\
&\le\quad c\,\|\lambda - \lambda_{\widetilde{h}}\|_{-1/2,\Gamma} \left\{ \sum_{e\in\mathcal{E}_h(\Gamma)} h_e\,\|\chi_e\|_{0,e}^2 \right\}^{1/2},
\end{aligned}
$$

from which the corresponding component of the efficiency estimate becomes $\|\lambda - \lambda_{\widetilde{h}}\|_{-1/2,\Gamma}$, thus finishing the proof. □

We end this section by remarking that the efficiency of $\boldsymbol{\theta}$ (cf. eq. (3.30) in Theorem 3.13) is now a straightforward consequence of Lemmas 3.14, 3.15, 3.18, 3.19, and 3.20. In turn, we emphasize that the resulting positive multiplicative constant, denoted by $C_{\texttt{eff}}$, is independent of h and $\widetilde{h}$.

3.4 Extension to the three–dimensional setting

In this section we explain how to adapt the a posteriori error analysis carried out so far for $n = 2$ to the three-dimensional case. In this way, we assume now that the partition $\mathcal{T}_h$ is a tetrahedral mesh of $\overline{\Omega}$, and we still denote by $\mathcal{E}$ (resp. $\mathcal{E}_h(\Omega)$, $\mathcal{E}_h(\Gamma)$, $\mathcal{E}_{h,T}(\Omega)$ and $\mathcal{E}_{h,T}(\Gamma)$) the set of all the associated faces (resp. internal faces, and on the boundary), like in the preliminaries introduced at the beginning of Section 3.

Additionally, we define the i-th row of the curl operator and the tangential component of matrix–valued functions $\boldsymbol{\zeta} = (\zeta_{i,j})_{1\le i,j\le 3}$, respectively as

$$[\,\mathrm{curl}(\boldsymbol{\zeta})\,]_i \;=\; \mathrm{curl}(\zeta_{i,1},\zeta_{i,2},\zeta_{i,3}), \quad \text{and} \quad [\,\boldsymbol{\zeta}\times\boldsymbol{\nu}\,]_i \;=\; (\zeta_{i,1},\zeta_{i,2},\zeta_{i,3})\times\boldsymbol{\nu}\,, \quad \text{for each } i=1,2,3,$$

where as usual

$$\underline{\mathbf{curl}}(\boldsymbol{\psi}) \;=\; \Big(\frac{\partial\psi_3}{\partial x_2} - \frac{\partial\psi_2}{\partial x_3}\,,\,\frac{\partial\psi_1}{\partial x_3} - \frac{\partial\psi_3}{\partial x_1}\,,\,\frac{\partial\psi_2}{\partial x_1} - \frac{\partial\psi_1}{\partial x_2}\Big) \quad \forall\,\psi=(\psi_1,\psi_2,\psi_3)\,.$$

Then, the local indicator $\boldsymbol{\theta}_T$ defining $\boldsymbol{\theta}^2 \;:=\; \sum_{T\in\mathcal{T}_h}\boldsymbol{\theta}_T^2 \,+\, \|\varphi_h-\varphi_D\|^2_{1/2,\Gamma}$, now reads

$$\begin{aligned}
\boldsymbol{\theta}_T^2 \;:=\;& \|\mu\,\nabla\boldsymbol{u}_h - \boldsymbol{\sigma}_h^{\mathrm{d}} - (\boldsymbol{u}_h\otimes\boldsymbol{u}_h)^{\mathrm{d}}\|^2_{0,T} \,+\, \|\mathbf{div}\,\boldsymbol{\sigma}_h + \varphi_h\,\boldsymbol{g}\|^2_{0,T}\\
&+\; h_T^2\,\|\mathrm{div}(\mathbb{K}\nabla\varphi_h) \,-\, \boldsymbol{u}_h\cdot\nabla\varphi_h\|^2_{0,T} \,+\, h_T^2\,\|\mathrm{curl}\big((\boldsymbol{\sigma}_h+\boldsymbol{u}_h\otimes\boldsymbol{u}_h)^{\mathrm{d}}\big)\|^2_{0,T}\\
&+\; \sum_{e\in\mathcal{E}_{h,T}(\Omega)}\Big\{h_e\,\|[\![(\boldsymbol{\sigma}_h+\boldsymbol{u}_h\otimes\boldsymbol{u}_h)^{\mathrm{d}}\times\boldsymbol{\nu}]\!]\|^2_{0,e} + h_e\,\|[\![\mathbb{K}\nabla\varphi_h\cdot\boldsymbol{\nu}]\!]\|^2_{0,e}\Big\}\\
&+\; \sum_{e\in\mathcal{E}_{h,T}(\Gamma)}\Big\{\|\boldsymbol{u}_D-\boldsymbol{u}_h\|^2_{0,e} \,+\, h_e\|\lambda_{\widetilde{h}} + \mathbb{K}\nabla\varphi_h\cdot\boldsymbol{\nu}\|^2_{0,e}\Big\}\\
&+\; \sum_{e\in\mathcal{E}_{h,T}(\Gamma)} h_e\Big\|(\boldsymbol{\sigma}_h \,+\, \boldsymbol{u}_h\otimes\boldsymbol{u}_h)^{\mathrm{d}}\times\boldsymbol{\nu} \,-\, \mu\nabla\boldsymbol{u}_D\times\boldsymbol{\nu}\Big\|^2_{0,e}\,.
\end{aligned} \tag{3.62}$$

The reliability and efficiency of $\boldsymbol{\theta}$ follows by slightly adapting the arguments employed for the $2d$−case. For instance, the Helmholtz decomposition of the space $\mathbb{H}_0(\mathbf{div};\Omega)$ required in Section 3.2.2 is guaranteed in this case by [15, Theorem 3.1], regardless the domain is convex or not, and all the arguments remain unchanged except the proof of Lemma 3.10. Here, such as in [17, Lemma 4.4], one needs to use the identity $\mathrm{curl}(\boldsymbol{\zeta})\boldsymbol{\nu} = \mathbf{div}(\boldsymbol{\zeta}\times\boldsymbol{\nu})$ for all $\boldsymbol{\zeta}\in\mathbb{H}^1(\Omega)$, and an integration by parts formula on the boundary to obtain

$$\mu\,\langle\,\mathrm{curl}(\boldsymbol{\phi}-I_h\boldsymbol{\phi})\,\boldsymbol{\nu}\,,\boldsymbol{u}_D\,\rangle_\Gamma \;=\; \int_\Gamma(\mu\,\nabla\boldsymbol{u}_D\times\boldsymbol{\nu})\;:\;(\boldsymbol{\phi}-I_h\boldsymbol{\phi})\,. \tag{3.63}$$

Also, integrating by parts on each element easily gives

$$\begin{aligned}
-\int_\Omega&\big(\boldsymbol{\sigma}_h+\boldsymbol{u}_h\otimes\boldsymbol{u}_h\big)^{\mathrm{d}} : \mathrm{curl}(\boldsymbol{\phi}-I_h\boldsymbol{\phi})\\
&=\; -\sum_{T\in\mathcal{T}_h}\int_T \mathrm{curl}\big((\boldsymbol{\sigma}_h \,+\, \boldsymbol{u}_h\otimes\boldsymbol{u}_h)^{\mathrm{d}}\big) : (\boldsymbol{\phi}-I_h\boldsymbol{\phi})\\
&\quad-\; \sum_{e\in\mathcal{E}_h(\Omega)}\int_e [\![(\boldsymbol{\sigma}_h \,+\, \boldsymbol{u}_h\otimes\boldsymbol{u}_h)^{\mathrm{d}}\times\boldsymbol{s}]\!] \;:\; (\boldsymbol{\phi}-I_h\boldsymbol{\phi})\\
&\quad-\; \sum_{e\in\mathcal{E}_h(\Gamma)}\int_e (\boldsymbol{\sigma}_h \,+\, \boldsymbol{u}_h\otimes\boldsymbol{u}_h)^{\mathrm{d}}\times\boldsymbol{\nu} : (\boldsymbol{\phi}-I_h\boldsymbol{\phi})\,.
\end{aligned} \tag{3.64}$$

Therefore, combining (3.63)-(3.64) in the expression $\mathcal{R}_2^{\mathtt{f}}(\,\cdot\,)$, and using next the Cauchy-Schwarz inequality and the approximation properties of the Clement interpolant (cf. (3.6)), one arrives at the analogous estimate (3.24), with the terms $(\boldsymbol{\sigma}_h+\boldsymbol{u}_h\otimes\boldsymbol{u}_h)^{\mathrm{d}}\times\boldsymbol{\nu}$ and $(\boldsymbol{\sigma}_h+\boldsymbol{u}_h\otimes\boldsymbol{u}_h)^{\mathrm{d}}\times\boldsymbol{\nu} - \mu\nabla\boldsymbol{u}_D\times\boldsymbol{\nu}$ appearing in (3.62).

Finally, the efficiency property also follows from the fact that all the Sobolev embeddings used in Section 3.3 hold for $n=3$ as well, and using now in the proof of Lemma 3.15 the corresponding results from Lemmas 4.8, 4.9 and 4.10 in [17] instead of Lemmas 4.9, 4.10 and 4.15 in [19], respectively.

4 Numerical Results

Our objective here is to illustrate the properties of the a posteriori error estimator $\boldsymbol{\theta}$ (cf. (3.1)) studied in the previous sections via an associated adaptive algorithm. The experiments we report below are all implemented in the two-dimensional setting using the public domain finite element software *FreeFem++* which provides the automatic adaptation procedure tool `adaptmesh` [22].

According to the discussion at the end of section 3.1, instead of $\boldsymbol{\theta}$ we actually consider the indicator $\widetilde{\boldsymbol{\theta}}$ defined as

$$\widetilde{\boldsymbol{\theta}}^2 := \sum_{T\in\mathcal{T}_h} \widetilde{\boldsymbol{\theta}}_T^2 \quad \text{where} \quad \widetilde{\boldsymbol{\theta}}_T^2 = \boldsymbol{\theta}_T^2 + \sum_{e\in\mathcal{E}_{h,T}(\Gamma)} \|\varphi_h - \varphi_D\|_{1,e}^2 \,, \tag{4.1}$$

where $\boldsymbol{\theta}_T$ is given by (3.2). Observe from its own definition that, although the additional assumption $\varphi_D \in \mathrm{H}^1(\Gamma)$ is required now, $\widetilde{\boldsymbol{\theta}}$ becomes a fully local and computable estimator (in contrast with $\boldsymbol{\theta}$) and, like in [2, Section 4], an interpolation argument shows that

$$\|\varphi_h - \varphi_h\|_{1/2,\Gamma}^2 \le C\,\|\varphi_h - \varphi_h\|_{1,\Gamma}^2 = C \sum_{e\in\mathcal{E}_h(\Gamma)} \|\varphi_h - \varphi_h\|_{1,e}^2 \quad \text{for some} \quad C > 0\,,$$

which says that $\widetilde{\boldsymbol{\theta}}$ is in fact induced by $\boldsymbol{\theta}$ (cf. (3.1)). Moreover, by proceeding as in section 3.2, we can also deduce that $\widetilde{\boldsymbol{\theta}}$ is a reliable estimator, that is, it satisfies the estimation (3.3) with the same $C_{\rm rel} > 0$ up to another $h, \widetilde{h}-$independent multiplicative constant C. In turn, up to the last term in (4.1), we find that $\widetilde{\boldsymbol{\theta}}$ is efficient. However, numerical results below allow us to conjecture that this indicator actually satisfies both properties.

As usual, the errors and the experimental convergence rates will be computed as

$$\mathsf{e}(\boldsymbol{\sigma}) := \|\boldsymbol{\sigma} - \boldsymbol{\sigma}_h\|_{\mathbf{div};\Omega}\,, \quad \mathsf{e}(\boldsymbol{u}) := \|\boldsymbol{u} - \boldsymbol{u}_h\|_{1,\Omega}\,,$$

$$\mathsf{e}(\varphi) := \|\varphi - \varphi_h\|_{1,\Omega}\,, \quad \mathsf{e}(\lambda) := \|\lambda - \lambda_h\|_{0,\Gamma}$$

and

$$r(\boldsymbol{\sigma}) := \frac{-2\log(\mathsf{e}(\boldsymbol{\sigma})/\mathsf{e}'(\boldsymbol{\sigma}))}{\log(N/N')}\,, \quad r(\boldsymbol{u}) := \frac{-2\log(\mathsf{e}(\boldsymbol{u})/\mathsf{e}'(\boldsymbol{u}))}{\log(N/N')}$$

$$r(\varphi) := \frac{-2\log(\mathsf{e}(\varphi)/\mathsf{e}'(\varphi))}{\log(N/N')}\,, \quad r(\lambda) := \frac{-2\log(\mathsf{e}(\lambda)/\mathsf{e}'(\lambda))}{\log(N/N')}\,,$$

where N and N' denote the total degrees of freedom associated to two consecutive triangulations with errors e and e'. In turn, the total error and the effectivity index associated to the global estimator $\widetilde{\boldsymbol{\theta}}$ are denoted and defined, respectively, as

$$\mathsf{e} = \left\{ \mathsf{e}(\boldsymbol{\sigma})^2 + \mathsf{e}(\boldsymbol{u})^2 + \mathsf{e}(\varphi)^2 + \mathsf{e}(\lambda)^2 \right\}^{1/2}\,, \quad \text{and} \quad \mathtt{eff}(\widetilde{\boldsymbol{\theta}}) = \frac{\mathsf{e}}{\widetilde{\boldsymbol{\theta}}}\,.$$

Test 1: accuracy assessment.

In our first example we illustrate the performance of the adaptive algorithm by considering a benchmark test for the Navier-Stokes equations in the domain $\Omega := (-1/2, 3/2) \times (0, 2)$ obtained by Kovasznay [23], which we also tested in our previous work [8] without adaptivity. The solution $(\boldsymbol{u}, p)$ is given by

$$\boldsymbol{u}(x_1, x_2) = \begin{pmatrix} 1 - e^{\vartheta x_1}\cos(2\pi x_2) \\ \frac{\vartheta}{2\pi} e^{\vartheta x_1}\sin(2\pi x_2) \end{pmatrix}, \qquad \text{and} \quad p(x_1, x_2) = -\tfrac{1}{2} e^{2\vartheta x_1} + \bar{p}\,,$$

where $\vartheta := \frac{-8\pi^2}{\mu^{-1}+\sqrt{\mu^{-2}+16\pi^2}}$ and the constant $\bar{p}$ is such that $\int_\Omega p = 0$. Note that the pressure p has a boundary layer at $\{-1/2\} \times (0,2)$, and the terms at the right-hand sides of the Boussinesq problem (1.1) are defined so that $(\boldsymbol{u}, p, \varphi)$ is the corresponding exact solution, with $\varphi(x_1, x_2) = x_1^2(x_2^2+1)$, and the data $\mu = 1$, $\mathbb{K} = e^{x_1+x_2}\mathbb{I}\ \forall\,(x_1,x_2) \in \Omega$, and $\mathbf{g} = (0,-1)^t$.

In Table 1 we present the numerical results reported in [8, Table I, Section VI] by using our augmented mixed-primal method via quasi–uniform refinements, and the corresponding results that we have obtained now by adaptivity, both for the finite element families $\mathbb{RT}_0 - \mathbf{P}_1 - \mathrm{P}_1 - \mathrm{P}_0$ $(k=0)$ and $\mathbb{RT}_1 - \mathbf{P}_2 - \mathrm{P}_2 - \mathrm{P}_1$ $(k=1)$. We notice that in each case the effective indexes $\mathtt{eff}(\widetilde{\boldsymbol{\theta}})$ remain always bounded and that the errors of the adaptive procedures decrease much faster than those obtained by the quasi–uniform ones. Particularly, the reduction of the computational cost by adaptivity can be much better observed in Figure 1 where we plot the total error $\mathtt{e}$ versus the degrees of freedom N for both refinement strategies. In figure 2, we display a refined mesh obtained in the sixth iterative adaptive procedure with $k=0$ when $N = 20762$, and observe there how the adaptive method is also able to recognize the region where the pressure has the aforementioned boundary layer.

Finally, in order to study the performance of the adaptive technique with respect to the stabilization parameters, we now take $\kappa_1 = \mu/2^n$ $(n = 1, \cdots, 4)$, chose κ_2 and κ_3 optimally (cf. (2.10)), compute the total errors with a quasi–uniform mesh with $N = 44313$ and present the corresponding results in Table 2 (see also [8, Table II]). We observe there that the errors remain bounded around $\mathtt{e} \approx 17$. Using adaptive procedures, we now examine, on the one hand, the number of degrees of freedom required to obtain an approximate total error to 17, summarize them in Table 3 (second row) and realize that no more than $N = 4000$ degrees of freedom are needed. On the other hand, we further compute the corresponding errors obtained with an adapted mesh with $N = 33873$ (the closer from below to $N = 44313$ degrees of freedom), display them in table 3 (third row) and find out in each case that the error is always lower than $\mathtt{e} \approx 6$. These results illustrate that the proposed adaptive algorithm has also improved the accuracy and the robustness of the numerical approximation driven by our augmented mixed-primal technique with regard to the stabilization parameters.

Test 2: adaptivity in a non-convex domain

Our second example focuses on the case where, under uniform mesh refinement, the convergence rates are affected by the loss of regularity of the exact solution. We set the problem on the L–shaped domain $\Omega = [-1,1]^2 \setminus [0,1]^2$, with the exact solutions given by

$$u(x_1,x_2) = \begin{pmatrix} -\cos(\pi x_1)\sin(\pi x_2) \\ \cos(\pi x_2)\sin(\pi x_1) \end{pmatrix}, \quad p(x_1,x_2) = \frac{1}{x_2+1.1} - \frac{1}{3}\ln(231)$$

$$\text{and} \quad \varphi(x_1,x_2) = \frac{x_2}{(x_1-0.15)^2+(x_2-0.15)^2}.$$

In turn, the data are given by $\nu = 0.5$, $\mathbb{K} = 0.75\mathbb{I}$ and $\boldsymbol{g} = (0,-1)^{\mathtt{t}}$, and the stabilization parameters are optimally chosen according to (2.10). Observe that the pressure and the temperature are singular along $x_2 = -1.1$ and in the point $(0.15, 0.15)$, respectively. In Table 4 we present the convergence history by quasi–uniform refinements and by adapted meshes according to the indicator $\widetilde{\boldsymbol{\theta}}$, and using the lowest family of finite element spaces $\mathbb{RT}_0 - \mathbf{P}_1 - \mathrm{P}_1 - \mathrm{P}_0$. As expected, we observe that the errors decrease faster through the adaptive procedure (see also Figure 3), and that in each case the effectivity indexes remain bounded. In Figure 4 we display some adapted meshes obtained during the adaptive refinement and observe that they are concentrated around $(0,0)$ and the line $x_2 = -1.1$, which illustrate again how the method is able to identify the regions in which the accuracy of the

N	$e(\boldsymbol{\sigma})$	$r(\boldsymbol{\sigma})$	$e(\boldsymbol{u})$	$r(\boldsymbol{u})$	$e(\varphi)$	$r(\varphi)$	$e(\lambda)$	$r(\lambda)$	$\mathtt{e}$	$\widetilde{\boldsymbol{\theta}}$	$\mathtt{eff}(\widetilde{\boldsymbol{\theta}})$
Mixed–primal $\mathbb{RT}_0 - \mathbf{P}_1 - \mathrm{P}_1 - \mathrm{P}_0$ scheme with quasi-uniform refinement											
806	73.0680	–	39.1463	–	1.3109	–	88.1781	–	121.0308	200.7144	0.6030
2934	44.1852	0.7786	21.5882	0.9213	0.5472	1.3524	45.3437	1.0295	66.8934	120.3119	0.5560
11321	24.3903	0.8801	11.3580	0.9512	0.2581	1.1130	22.1691	1.0599	34.8630	64.0981	0.5439
44313	11.6299	1.0854	5.2548	1.1297	0.1305	0.9995	10.8290	1.0501	16.7377	30.9900	0.5401
177320	5.7070	1.0268	2.5486	1.0436	0.0639	1.0299	5.3797	1.0090	8.2468	15.2465	0.5409
700032	2.8348	1.0191	1.2442	1.0444	0.0318	1.0164	2.6694	1.0297	4.0879	7.5547	0.5411
Mixed–primal $\mathbb{RT}_0 - \mathbf{P}_1 - \mathrm{P}_1 - \mathrm{P}_0$ scheme with adaptive refinement according to $\widetilde{\boldsymbol{\theta}}$											
744	75.4832	–	38.5758	–	2.0214	–	4.1769	–	84.8960	168.1490	0.5049
1739	33.7108	1.8989	15.3418	2.1720	0.9529	1.7716	2.1230	1.5942	37.1107	119.6710	0.3101
4058	14.8804	1.9301	8.5433	1.3818	0.9929	-0.1091	2.6746	-0.5451	17.3943	70.3655	0.2472
7279	10.7673	1.1074	6.7981	0.7821	0.9877	0.0353	2.1344	0.7722	12.9491	52.3409	0.2474
12724	7.8346	1.1386	4.7949	1.2501	0.8924	0.3634	1.3313	1.6902	9.3243	37.7500	0.2470
20762	6.1931	0.9604	3.7492	1.0049	0.6927	1.0345	0.8424	1.8695	7.3212	29.6167	0.2472
33873	4.8417	1.0058	3.0095	0.8980	0.5960	0.6149	0.6218	1.2408	5.7655	23.3614	0.2468
53405	3.8966	0.9540	2.4360	0.9287	0.4569	1.1671	0.4782	1.1532	4.6428	18.7966	0.2470
87163	3.0914	0.9450	1.8660	1.0883	0.3499	1.0898	0.3313	1.4985	3.6430	14.7548	0.2469
Mixed–primal $\mathbb{RT}_1 - \mathbf{P}_2 - \mathrm{P}_2 - \mathrm{P}_1$ scheme with quasi-uniform refinement											
2686	28.7886	–	9.9080	–	0.1358	–	10.0095	–	32.0493	54.5149	0.5879
10078	9.0869	1.7441	3.2510	1.6855	0.0240	2.6214	2.5666	2.0585	9.9864	17.5231	0.5699
39550	2.5644	1.8506	0.8685	1.9309	0.0045	2.4487	0.6438	2.0230	2.7830	4.8849	0.5697
156158	0.5872	2.1468	0.1913	2.2033	0.0009	2.3439	0.1609	2.0194	0.6382	1.1200	0.5698
627578	0.1429	2.0319	0.0442	2.1066	0.0002	2.1626	0.0402	1.9941	0.1549	0.2717	0.5699
Mixed–primal $\mathbb{RT}_1 - \mathbf{P}_2 - \mathrm{P}_2 - \mathrm{P}_1$ scheme with adaptive refinement according to $\widetilde{\boldsymbol{\theta}}$											
2493	32.4117	–	10.9303	–	1.0840	–	0.5708	–	34.2270	166.4739	0.2056
5428	5.4016	4.6057	1.9844	4.3857	1.0020	0.2022	0.1402	3.6084	5.8428	30.9143	0.1890
12039	1.6132	3.0342	1.0296	1.6474	0.6655	1.0293	0.1302	0.1869	2.0302	9.8028	0.2071
21884	0.9283	1.8494	0.6120	1.7412	0.4530	1.2848	0.0979	0.9548	1.2046	4.6925	0.2567
36867	0.5456	1.9385	0.3582	1.9539	0.2700	1.8875	0.0602	1.7720	0.7089	1.9685	0.3601
69946	0.2780	2.1976	0.2098	1.7434	0.1503	1.9092	0.0297	2.2985	0.3805	1.0516	0.3618
118901	0.1690	1.8762	0.1278	1.8682	0.0876	2.0350	0.0172	2.0641	0.2299	0.6349	0.3621
202131	0.1002	1.9702	0.0730	2.1107	0.0471	2.3388	0.0098	2.1202	0.1330	0.3671	0.3622

Table 1: TEST 1: Convergence history and effectivity indexes for the mixed–primal approximation of the Boussinesq problem under quasi-uniform, and adaptive refinement according to the indicator $\widetilde{\boldsymbol{\theta}}$.

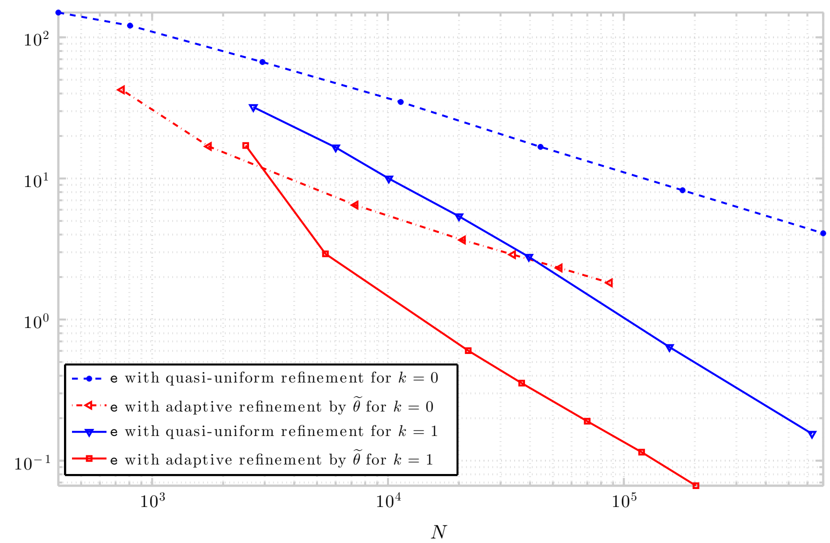

Figure 1: Test 1: Decay of the total error with respect to the number of degrees of freedom using quasi-uniform and adaptive refinement strategies for both $k = 0$ and $k = 1$.

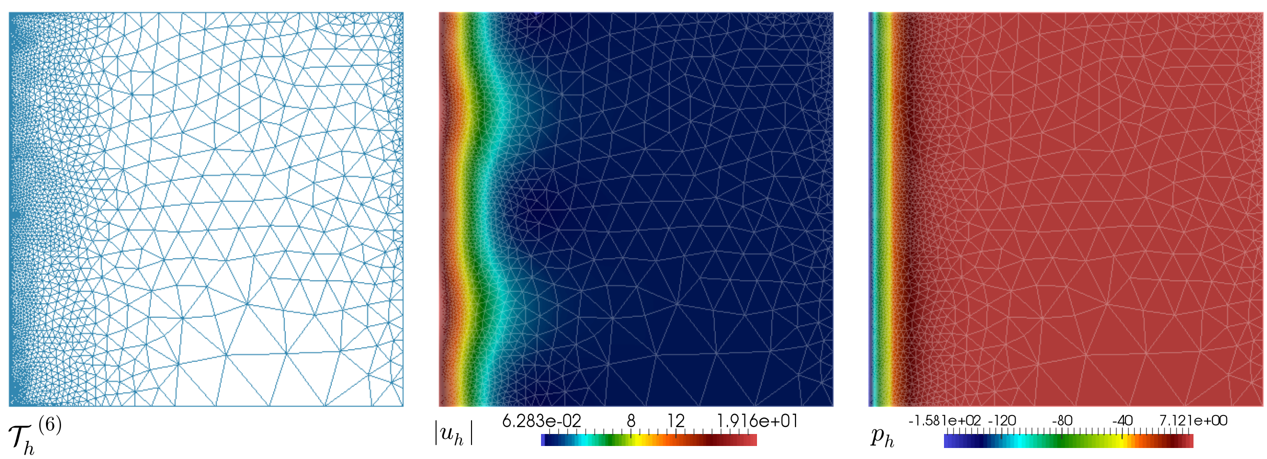

Figure 2: Test 1: Snapshots of an adapted mesh in the sixth iteration refinement (left), and over this triangulation the approximate velocity magnitude (center) and the postprocessed pressure (left) with the proposed lowest order mixed-primal method.

κ_1	μ	$\mu/2$	$\mu/4$	$\mu/8$	$\mu/16$
e	16.7371	16.7381	16.7390	16.7392	16.77391

Table 2: Test 1: κ_1 vs. $\mathsf{e}(\boldsymbol{\sigma}, \boldsymbol{u}, \varphi, \lambda)$ for the mixed $\mathbb{RT}_0 - \mathbf{P}_1 - \mathrm{P}_1 - \mathrm{P}_0$ approximation of the Boussinesq equations with a quasi-uniform mesh with $N = 44313$ and $\mu = 1$.

κ_1	μ	$\mu/2$	$\mu/4$	$\mu/8$	$\mu/16$
Required N by adapted procedures with $\mathsf{e} \approx 17$	4058	3936	3882	3830	3803
Associated e to an adapted mesh with $N = 33873$	5.7655	5.6291	5.6321	5.6352	5.6251

Table 3: Test 1: κ_1 vs. required number of degrees of freedom N via adaptive procedures for an error around $\mathsf{e} \approx 17$ (2nd. row) and κ_1 vs. total error obtained via an adapted mesh with $N = 33873$ (3rd. row) using the $\mathbb{RT}_0 - \mathbf{P}_1 - \mathrm{P}_1 - \mathrm{P}_0$ approximation of the Boussinesq equations and $\mu = 1$.

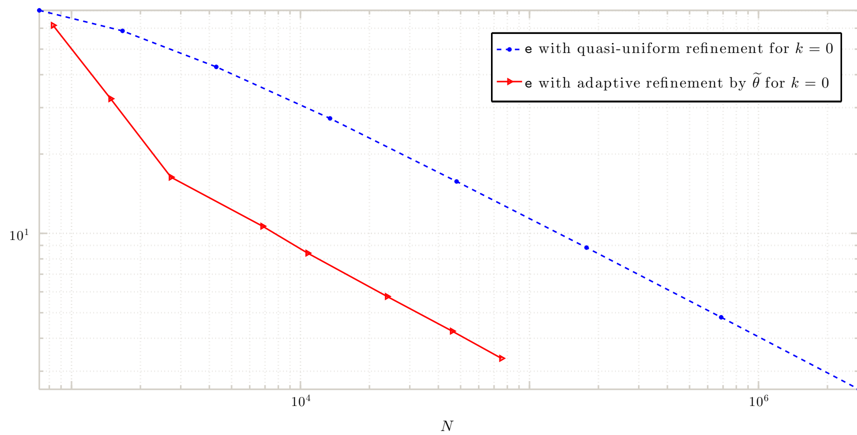

Figure 3: Test 2: Decay of the total error with respect to the number of degrees of freedom using quasi-uniform and adaptive refinement strategies for $k = 0$.

numerical approximation is deteriorated. To visualize better the latter statement, we have displayed in Figure 5 the approximate pressure and the approximate temperature obtained in the $10th$ adaptive iteration.

References

[1] K. Allali, *A priori and a posteriori error estimates for Boussinesq equations.* Int. J. Numer. Anal. Model. 2 (2005), no. 2, 179–196.

[2] M. Álvarez, G.N. Gatica and R. Ruíz–Baier, *A posteriori error analysis for a viscous flow–transport problem.* ESAIM Math. Model. Numer. Anal. 50 (2016), no. 6, 1789–1816.

[3] C. Bernardi, B. Métivet, B. Pernaud-Thomas, *Couplage des équations de Navier-Stokes et de la chaleur: le modèle et son approximation par éléments finis.* RAIRO Modl. Math. Anal. Numér. 29 (1995), no. 7, 871–921.

[4] F. Brezzi and M. Fortin, *Mixed and Hybrid Finite Element Methods.* Springer-Verlag, 1991.

[5] P.G. Clément, *Approximations by finite element functions using local regularization.* RAIRO Modl. Math. Anal. Numér. 9 (1975), 77–84.

[6] A. Çibik, K. Songül, *A projection-based stabilized finite element method for steady-state natural convection problem.* J. Math. Anal. Appl. 381 (2011), 469–484.

N	$e(\boldsymbol{\sigma})$	$r(\boldsymbol{\sigma})$	$e(\boldsymbol{u})$	$r(\boldsymbol{u})$	$e(\varphi)$	$r(\varphi)$	$e(\lambda)$	$r(\lambda)$	$\mathtt{e}$	$\widetilde{\boldsymbol{\theta}}$	$\mathtt{eff}(\widetilde{\boldsymbol{\theta}})$
Mixed–primal $\mathbb{RT}_0 - \mathbf{P}_1 - \mathrm{P}_1 - \mathrm{P}_0$ scheme with quasi-uniform refinement											
723	14.8755	–	1.8533	–	67.9954	–	8.4392	–	70.1378	76.2146	0.9203
1671	11.8135	0.5502	1.2108	1.0162	57.0961	0.4171	6.0269	0.8037	58.6286	63.3184	0.9255
4287	8.7667	0.6332	0.7247	1.0897	41.6790	0.6681	4.2077	0.7627	42.8045	46.3784	0.9225
13455	6.4965	0.5240	0.4005	1.0371	26.3907	0.7991	2.4929	0.7154	27.2916	28.6658	0.9522
48027	5.1180	0.3749	0.2091	1.0215	14.8104	0.9080	1.4370	0.8659	15.7369	16.5554	0.9517
177459	3.8766	0.4251	0.1071	1.240	7.9018	0.9614	0.7141	1.0701	8.8311	9.2683	0.9528
686823	2.5643	0.6107	0.0541	1.0086	4.0438	0.9900	0.3780	0.9401	4.8035	5.0883	0.9553
2741390	1.5678	0.7109	0.0273	0.9905	2.0174	1.0047	0.1862	1.0233	2.5619	2.6910	0.9520
Mixed–primal $\mathbb{RT}_0 - \mathbf{P}_1 - \mathrm{P}_1 - \mathrm{P}_0$ scheme with adaptive refinement according to $\widetilde{\boldsymbol{\theta}}$											
831	13.899	–	1.6294	–	59.5034	–	7.2295	–	61.5531	65.8293	0.9351
1482	12.7555	0.2970	1.4798	0.3329	29.6098	2.4128	3.2038	2.8135	32.4330	35.6381	0.9101
2718	9.9315	0.8252	1.3452	0.3145	12.7939	2.7671	1.5892	2.3120	16.3296	18.3478	0.8900
4164	8.9724	0.4762	1.2689	0.2739	9.3464	1.4721	1.3453	0.7811	13.0873	15.5884	0.8971
6831	6.9905	1.0085	0.8927	1.7165	7.9239	0.6671	0.9929	1.2271	10.6456	11.7306	0.9075
10743	5.9708	0.6907	0.7359	0.5300	5.8156	1.3664	0.8512	1.6803	8.4161	9.2616	0.9087
17763	5.0023	0.7090	0.5847	0.9148	4.6198	0.9156	0.6170	1.2800	6.8620	7.5482	0.9091
27888	4.2234	0.7505	0.4219	1.4471	3.8638	0.7923	0.5160	0.7923	5.7629	6.3419	0.9087
45930	3.0992	1.2407	0.3568	0.6712	2.8701	1.1918	0.3883	1.1395	4.2568	4.7103	0.9037
75408	2.9371	1.0363	0.2737	1.0699	2.31245	0.8715	0.3108	0.8978	3.3563	3.6888	0.9099

Table 4: TEST 2: Convergence history and effectivity indexes for the mixed–primal approximation of the Boussinesq problem under quasi-uniform, and adaptive refinement according to the indicator $\widetilde{\boldsymbol{\theta}}$.

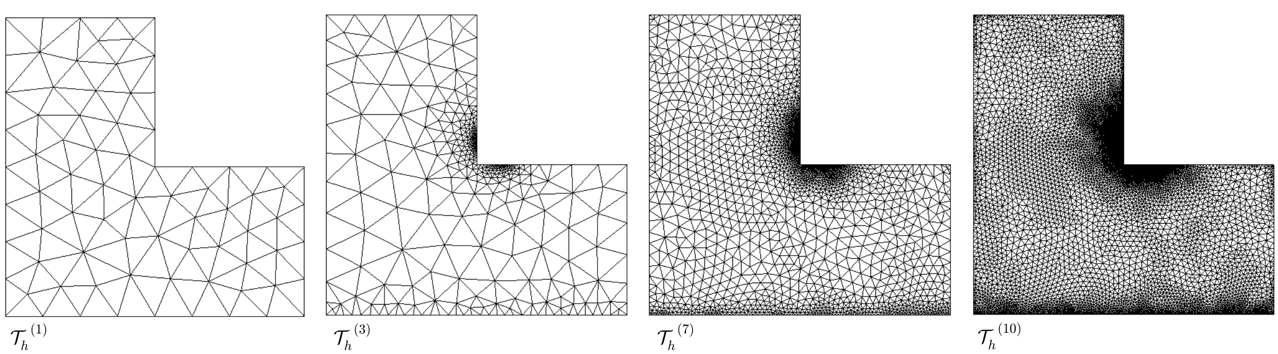

Figure 4: TEST 2: Snapshots of adapted meshes according to the indicator $\widetilde{\boldsymbol{\theta}}$.

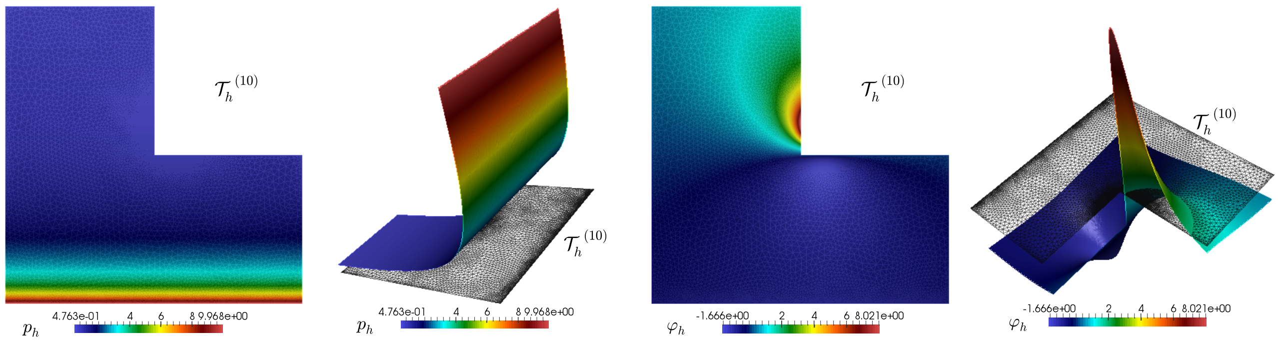

Figure 5: Test 2: Approximate pressure p_h and temperature φ_h in the L-shaped domain over an adapted mesh obtained via the estimator $\widetilde{\boldsymbol{\theta}}$ using the mixed-primal family $\mathbb{RT}_0 - \mathbf{P}_1 - \mathrm{P}_1 - \mathrm{P}_0$.

[7] E. Colmenares, G.N. Gatica and R. Oyarzúa, *An augmented fully-mixed finite element method for the stationary Boussinesq problem*. Calcolo, to appear. DOI: 10.1007/s10092-016-0182-3.

[8] E. Colmenares, G.N. Gatica and R. Oyarzúa, *Analysis of an augmented mixed–primal formulation for the stationary Boussinesq problem.* Numer. Methods Partial Differential Equations 32 (2016), no. 2, 445–478.

[9] E. Colmenares, G.N. Gatica and R. Oyarzúa, *Fixed point strategies for mixed variational formulations of the stationary Boussinesq problem.* C.R. Math. Acad. Sci. Paris 354 (2016), no. 1, 57–62.

[10] E. Colmenares, M. Neilan, *Dual–mixed formulations for the stationary Boussinesq problem.* Comp. Math. Appl. 72 (2016), no. 7, 1828–1850.

[11] M. Farhloul, S. Nicaise and L. Paquet *A mixed formulation of Boussinesq equations: analysis of nonsingular solutions.* Math. Comp. 69 (2000), no. 231, 965–986.

[12] M. Farhloul, S. Nicaise and L. Paquet, *A refined mixed finite element method for the Boussinesq equations in polygonal domains.* IMA J. Numer. Anal. 21 (2001), no. 2, 525–551.

[13] G.N. Gatica, *A note on the efficiency of residual-based a-posteriori error estimators for some mixed finite element methods*. Electron. Trans. Numer. Anal. 17 (2004), 218–233.

[14] G.N. Gatica, *A Simple Introduction to the Mixed Finite Element Method: Theory and Applications*. Springer Briefs in Mathematics. Springer, Cham, 2014.

[15] G.N. Gatica, *A note on stable Helmholtz decompositions in 3D.* Preprint 2016-03, Centro de Investigacion en Ingenieria Matematica (CI^{2}MA), Universidad de Concepcion, Chile, (2016).

[16] G.N. Gatica, L.F. Gatica and A. Márquez, *Analysis of a pseudostress-based mixed finite element method for the Brinkman model of porous media flow*. Numer. Math. 126 (2014), no. 4, 635–677.

[17] G.N. Gatica, L.F. Gatica and F.A. Sequeira, *A priori and a posteriori error analyses of a pseudostress-based mixed formulation for linear elasticity.* Comp. Math. Appl. 71 (2016), no. 2, 585–614.

[18] G.N. Gatica, G.C. Hsiao and S. Meddahi, *A residual–based a posteriori error estimator for a two-dimensional fluid-solid interaction problem.* Numer. Math. 114 (2009), no. 1, 63–106.

[19] G.N. Gatica, A. Márquez and M.A. Sánchez, *Analysis of a velocity–pressure–pseudostress formulation for the stationary Stokes equations*. Comput. Methods Appl. Mech. Engrg. 199 (2010), no. 17-20, 1064–1079.

[20] G.N. Gatica, A. Márquez and M.A. Sánchez, *A priori and a posteriori error analyses of a velocity–pseudostress formulation for a class of quasi–Newtonian Stokes flows.* Comput. Methods Appl. Mech. Engrg. 200 (2011), no. 17-20, 1619–1636.

[21] G.N. Gatica, R. Ruiz-Baier and G. Tierra, *A posteriori error analysis of an augmented mixed method for the Navier–Stokes equations with nonlinear viscosity.* Comp. Math. Appl. 72 (2016), no. 9, 2289–2310.

[22] F. Hecht, *New development in FreeFem++.* J. Numer. Math. 20 (2012), no. 3-4, 251–265.

[23] L. I. G. Kovasznay, *Laminar flow behind a two-dimensional grid.* Math. Proc. Cambridge Philos. Soc. 44 (1948), 58–62.

[24] S.A. Lorca and J. L. Boldrini, *Stationary solutions for generalized Boussinesq models.* J. Differential Equations 124 (1996), no. 2, 389–406.

[25] H. Morimoto, *On the existence and uniqueness of the stationary solution to the equations of natural convection.* Tokyo J. Math. 14 (1991), 220–226.

[26] H. Morimoto, *On the existence of weak solutions of equation of natural convection.* J. Fac. Sci., Univ. Tokyo, Sect. 1A, Math. 36 (1989), 87–102.

[27] R. Oyarzúa, T. Qin and D. Schötzau, *An exactly divergence-free finite element method for a generalized Boussinesq problem.* IMA J. Numer. Anal. 34 (2014), no. 3, 1104–1135.

[28] R. Oyarzúa, P. Zuñiga, *Analysis of a conforming finite element method for the Boussinesq problem with temperature-dependent parameters.* Preprint 2015-27, Centro de Investigación en Ingeniería Matemática (CI^2MA), Universidad de Concepción, Chile, (2015).

[29] P.H. Rabinowitz, *Existence and nonuniqueness of rectangular solutions of the Bénard problem.* Arch. Ration. Mech. Anal. 29 (1968), 32–57.

[30] E.L. Reiss and J. Tavantzis, *A boundary value problem of thermal convection.* J. Differential Equations 35 (1980), no. 9, 45–54.

[31] J.E. Roberts and J.M. Thomas, *Mixed and Hybrid Methods.* In: Handbook of Numerical Analysis, P.G. Ciarlet and J.L. Lions (Eds.), vol. II, Finite Element Methods (Part 1), North-Holland, Amsterdam, 1991.

[32] D. J. Tritton, *Physical Fluid Dynamics.* NeVan Nostrand Reinhold Co., New York, 1977

[33] R. Verfürth, *A Posteriori Error Estimation Techniques for Finite Element Methods. Numerical Mathematics and Scientific Computation*, Oxford University Press, 2013.

[34] R. Verfürth, *A posteriori error estimates for nonlinear problems: finite element discretizations of elliptic equations.* Math. Comp 62 (1994), 445–475.

[35] Y. Zhang, Y. Hou, H. Zuo. *A posteriori error estimation and adaptive computation of conduction convection problems.* Appl. Math. Model. 35 (2011), 2336–2347.

Centro de Investigación en Ingeniería Matemática (CI²MA)

PRE-PUBLICACIONES 2016

- 2016-26 Mario Álvarez, Gabriel N. Gatica, Ricardo Ruiz-Baier: *A posteriori error analysis for a sedimentation-consolidation system*
- 2016-27 Luis F. Gatica, Ricardo Oyarzúa, Nestor Sánchez: *A priori and a posteriori error analysis of an augmented mixed-FEM for the Navier-Stokes-Brinkman problem*
- 2016-28 Luci Fatori, Tais De Olivera Saito, Mauricio Sepúlveda, Eiji Renan Takahashi: *Energy decay to Timoshenko system with indefinite damping*
- 2016-29 Sophie Balemans, Raimund Bürger, Stefan Diehl, Pierre Francois, Julien Laurent, Florent Locatelli, María Carmen Martí, Ingmar Nopens, Elena Torfs, Peter Vanrolleghem: *Concentration-driven models revisited: Towards a unified framework to model settling tanks in water resource recovery facilities*
- 2016-30 Ernesto Cáceres, Gabriel N. Gatica, Filander A. Sequeira: *A mixed virtual element method for the Brinkman problem*
- 2016-31 Ana Alonso-Rodriguez, Jessika Camaño, Rodolfo Rodríguez, Alberto Valli, Pablo Venegas: *Finite element approximation of the spectrum of the curl operator in a multiply-connected domain*
- 2016-32 David Mora, Gonzalo Rivera, Rodolfo Rodríguez: *A posteriori error estimates for a virtual elements method for the Steklov eigenvalue problem*
- 2016-33 Raimund Bürger, Gerardo Chowell, Elvis Gavilán, Pep Mulet, Luis M. Villada: *Numerical solution of a spatio-temporal gender-structured model for hantavirus infection in rodents*
- 2016-34 Felipe Lepe, Salim Meddahi, David Mora, Rodolfo Rodríguez: *Acoustic vibration problem for dissipative fluids*
- 2016-35 Alfredo Bermúdez, Marta Piñeiro, Rodolfo Rodríguez, Pilar Salgado: *Analysis of an ungauged T,\phi - \phi formulation of the eddy current problem with currents and voltage excitations*
- 2016-36 Jessika Camaño, Ricardo Oyarzúa, Ricardo Ruiz-Baier, Giordano Tierra: *Error analysis of an augmented mixed method for the Navier-Stokes problem with mixed boundary conditions*
- 2016-37 Eligio Colmenares, Gabriel N. Gatica, Ricardo Oyarzúa: *A posteriori error analysis of an augmented mixed-primal formulation for the stationary Boussinesq model*

Para obtener copias de las Pre-Publicaciones, escribir o llamar a: Director, Centro de Investigación en Ingeniería Matemática, Universidad de Concepción, Casilla 160-C, Concepción, Chile, Tel.: 41-2661324, o bien, visitar la página web del centro: http://www.ci2ma.udec.cl




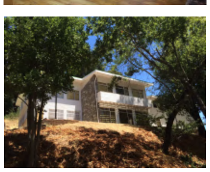

CENTRO DE INVESTIGACIÓN EN
INGENIERÍA MATEMÁTICA (CI^{2}MA)
Universidad de Concepción

Casilla 160-C, Concepción, Chile
Tel.: 56-41-2661324/2661554/2661316
http://www.ci2ma.udec.cl